Desalination and Water Treatment
www.deswater.com
doi: 10.5004/dwt.2022.28103

249 (2022) 1–22
February

Fouling and fouling mitigation in batch reverse osmosis: review and outlook

L. Burlace, P.A. Davies*

School of Engineering, University of Birmingham, Edgbaston, Birmingham, B15 2TT, UK,
emails: p.a.davies@bham.ac.uk (P.A. Davies), Lxb299@student.bham.ac.uk (L. Burlace)

Received 2 July 2021; Accepted 31 December 2021

ABSTRACT

In recent years, many advances have been made in reverse osmosis (RO) technology, and in understanding the fouling and scaling phenomena that limit its performance and durability. One of these advances, batch RO, is an unsteady process that has several flow characteristics that are absent in standard reverse osmosis processes. These include osmotic backwashing, feed flow reversal, salinity cycling and water hammer/pulse flow. This paper has three aims. First, it introduces batch RO and reviews recent progress in this area. Second, it reviews the fouling phenomena experienced in RO, covering the fouling mechanisms, detection methods currently in use, and mitigation methods already used in conventional RO. Lastly, it reviews specific flow characteristics experienced in batch reverse osmosis and it discusses the effects that they may have on the fouling. The paper concludes by recommending research activities to advance further batch RO technology for improved mitigation of fouling.

Keywords: Fouling; Fouling detection; Batch reverse osmosis; Osmotic backwash; Salinity cycling

1. Introduction

Water shortage is a growing global problem. Over 16% of the global population lacks access to clean sanitary water [1]. Treatment of secondary water sources, such as brackish groundwater and seawater, is becoming more common across the globe as a solution to this problem. Many secondary water sources require desalination before use. The preferred method of desalination is reverse osmosis (RO) due to its energy efficiency, high rejection potential and relatively small footprint [2]. May advances have been made in membrane technology over the previous decades, as well as improvements in methods of operating RO [3,4]. In recent years, extensive research has been conducted in the field of high recovery and low specific energy consumption (SEC) methods of RO, including batch reverse osmosis (BRO) [5–26].

BRO is a desalination process that allows the minimum energy required to reach the osmotic pressure to be applied at all times by varying the pressure over time. The process allows high recovery ratio and a low SEC, which is desirable as it reduces operational costs and allows more usable water to be generated per unit volume of source water. The SEC is defined as the amount of energy required to produce a volume of water and is typically stated in kWh/m^3, the recovery ratio is defined as the amount of potable water extracted from each batch of feed water.

The negative side to high recovery RO is that the membranes are subject to a highly concentrated solution. Depending on the composition of the source water, this introduces a danger of membrane fouling. Fouling is the process of organic or inorganic substances in the feed water precipitating on the membrane, blocking the pores and impairing performance [27]. Despite the growing number of papers on batch RO, only a few studies have been conducted on the fouling potential and mitigation of batch RO [12–16]. Unlike most conventional RO, batch RO is an unsteady process and therefore fouling tendency can

* Corresponding author.

be expected to differ. Thus, this paper aims to review the mechanisms of fouling, fouling detection methods and the potential mitigation of fouling that may take place during the batch RO process based on the studies of batch RO and related unsteady RO processes.

The structure of this paper is as follows, the BRO process is described in detail and key literature is highlighted. Then, fouling limitations of RO are reviewed, with attention paid to the mechanisms, detection methods and standard mitigation methods. This is then followed by a review of specific flow characteristics experienced during the BRO process that may have a propensity to reduce or remove fouling and scaling.

2. Batch RO concept

The rationale of using batch RO is that, in the ideal case, the minimum required pressure to drive water through the membrane need only be exceeded by a small margin — thus reducing excess pressure and wasted energy in comparison to a conventional multistage RO system. Batch RO is a cyclic process requiring an average pressure below that required by conventional RO. As in conventional RO, the performance of batch RO systems is typically expressed by two key parameters: the SEC and recovery ratio. Table 1 summarises the performance of a range of BRO systems. Many theoretical studies prove that batch RO can achieve a specific energy consumption near to the thermodynamic minimum energy required. A few practical studies, using bladder and free-piston versions of batch RO, confirm that high recovery ratios and low energy consumption are feasible [7,8,10,11,18,19]. Nonetheless, losses result in lower performance than the ideal case. The bladder BRO system achieved a SEC of 0.25 kWh/m^3 but with a recovery ratio less than 0.55, because operating conditions were limited by maximum operating pressure [10,19]. In contrast, the free moving piston system could achieve an SEC of 0.51–0.65 kWh/m^3 with a recovery ratio of 0.72 [11].

Batch RO differs from the related process of semi-batch RO in that the pressurised make up or feed solution is separated from the recirculating concentrate [26]. The two main methods of achieving this separation, that is, bladder separation [10] and free moving piston separation [11], are illustrated in Fig. 1.

These two methods work on similar principles. Both have two compartments (feed and batch) on the feed side of the membrane; and both have a productive (pressurisation) and a non-productive (refill or reset) stage as described in Fig. 1. During the production phase, the feed compartment of the system does not connect with the batch compartment. As the batch is processed, permeate leaves the system, while the concentrate is mixed back into the batch which increases the salinity of the batch thus increasing the osmotic pressure. In turn, the feed pressure also increases. In both methods, the recovery ratio is a function of the batch volume and the dead volume around the membrane and pipework. Higher recovery requires larger batch volume while dead volume should be minimised [11].

Towards the end of the batch process, the batch concentration can exceed the saturation index limit of any sparingly soluble salts in the feed solution. This can result in salt crystals forming on the membrane surface or on other suspended solids throughout the system. The batch time is important when predicting scaling in the RO process, because standard nucleation theory states that the saline solution must be supersaturated for a period before nucleation of sparingly soluble salts can take place, this is known as the induction time [28]. These scaling mechanisms are explained in more detail later in this review.

3. Types of fouling

This chapter will highlight the common types of fouling, describing the mechanisms of formation, causes of the different types of fouling and giving some examples of the types of fouling agents. Additionally, these will be linked to how these types of fouling may occur during the desalination process.

During fouling, suspended substances, such as soluble salts or biomatter present in the feed, precipitate onto the membrane surface and decrease membrane performance. Fouling can be divided in two categories, organic and inorganic. Organic fouling is the fouling caused by organic matter in the feed [29,30]. The organic matter can be in the form of bacteria, algae, proteins, humic substances, fatty acids, organic acids, cell compounds etc [30,31]. Inorganic fouling is the process of salt precipitation in the bulk solution (i.e., homogenous nucleation) or to the surface of the membrane or any other suspended solids in the feed solution (i.e., heterogenous nucleation). Within these two main categories of fouling, there are several subcategories as shown in Fig. 2. Organic fouling can be sub-divided into fouling by micro-organisms and macro-molecules (organic colloidal fouling) [32]. Inorganic fouling can also be sub-categorised as scaling by sparingly solution salts, and fouling by metal oxides (inorganic colloidal fouling) [27,30,31,33–36].

3.1. Micro-organism fouling mechanism

Organic fouling by micro-organisms occurs when the micro-organisms attach to the membrane surface and create a biofilm layer. The evolution of biofilm follows a two-stage process of adsorption/adhesion followed by growth [32,37].

3.1.1. Adsorption/Adhesion

There are two processes within the adsorption stage: the initial adhesion of micro-organisms to the pristine substrate (membrane surface) followed by additional micro-organisms adhering to the now conditioned surface. The initial adsorption involves organic molecules adhering to the pristine surface of the membrane. Once adhered, the micro-organisms secrete an extracellular polymeric substance (EPS) that facilitates subsequent attachment of micro-organisms [38]. The initial adsorption on the pristine surface is governed by macroscopic properties of the surface and bulk solution such as the electrokinetic (electronic charge) and hydrophobic (cell-water contact angle) properties these are known as non-specific conditions [39,40]. On the other hand, the interactions with the conditioned membrane surface are specific interactions. These are in the form of physio-chemical reactions such as Lifshitz-Van

Table 1
An overview of batch RO performance studies comparing SEC and recovery ratios

Type of system	Type of study (theoretical or experimental)	Focus of study	Feed water (ppm)	Recovery range (%)	SEC (kWh/m^3)	Notes	Reference
Batch RO with free moving piston	Theoretical with proof of concept	Designing a batch RO system with an efficiency approaching the theoretical minimum	Brackish (2,000–5,000 ppm)	30–70	0.196–0.323	Stated SEC is theoretical hydraulic SEC. Including pump efficiencies an expected SEC 0.6 kWh/m^3 can be expected	[20]
Batch RO with bladder	Theoretical with proof of concept	Designing and modelling a batch RO system using the innovative bladder system to reach the theoretical limits of efficiency	Theoretical study on seawater and brackish water. Model validation completed with brackish water (2,000–5,000 ppm)	<55	≈0.3	Theoretical model is within 3% of concept test results. Low recovery is due to limited pressure limitations. Pump efficiency is not included in these results	[19]
Variable volume feed tank batch RO (ideal batch). Batch RO using an ERD, semi-batch RO process	Theoretical	Can batch and semi-batch achieve similar performances to staged continuous RO	Seawater (35,040) and brackish water (5,840 ppm)	Seawater recovery was set to 50, BWRO recovery 90%	SWRO ideal batch 1.8 SWRO semi-batch 1.94 SWRO Batch with ERD 2.1 BWRO ideal batch 0.66 BWRO semi-batch 1.21 BWRO with ERD 0.74	All SEC's are assuming a pressure drop in the recirculation of 0.1 Bar. No pump efficiencies have been used in this model. ERD efficiency is 98%	[18]
Piston batch RO CCD-RO	Theoretical	Comparison of different arrangements of RO tech. CCD-RO and batch RO	Brackish (4,000ppm)	80%	CCD-RO 0.26 Batch RO 0.17	No practical design is displayed in this paper	[21]
Free piston steam operated batch RO	Experimental	Performance of a batch RO system and concentration polarisation	Brackish (2,500 ppm)	Not stated	Optimal 1.2 minimum approximately 0.95	This SEC includes inefficiencies such as the pump	[6]

(Continued)

Table 1 Continued

Type of system	Type of study (theoretical or experimental)	Focus of study	Feed water (ppm)	Recovery range (%)	SEC (kWh/m^3)	Notes	Reference
Free moving piston manually operated batch RO	Experimental	Analyse the performance of a batch RO system reaching the theoretical minimum energy required	Brackish (2,074–4,989 ppm)	40.3%–68.9%	0.135–0.337	This system was completely manual, the SEC is the pure hydraulic SEC	[20]
Bladder batch RO	Experimental and theoretical	Comparing the experimental results to the theoretical results of a batch RO system	Brackish (2,000–5,000 ppm)	<55%	0.25	System recovery ratio is limited by the maximum operating pressure being 10 Bar	[19]
Bladder batch RO	Experimental and theoretical	Model validation and predicted energy savings	Brackish (5,000 ppm), seawater (35,000 ppm)	Brackish 90%, seawater 50%	Brackish 0.91 Seawater 1.96	This system has not been tested past 50% recovery; the higher recovery data is predicted from the model	[10]
Bladder batch RO	Theoretical and experimental	Impacts of salt retention on batch RO	Seawater 35,000 ppm	50%	1.96	This study validates the model using brackish water, then makes predictions on energy savings for sea water	[22]
Free moving piston batch RO, single acting 3 stage, single acting 2 stage, double acting 2 stage, single acting 2 stage multi vessel	Experimental	Making a batch RO system that is suitable for off grid use using readily available components	Brackish 2,000 ppm	Single acting 3 stage 70% Single acting 2 stage 73% Double acting 76% Single acting 2 stage multi vessel 72%	Single acting 3 stage hydraulic 0.27 Single acting 2 stage hydraulic 0.36 Electrical 2.31 Double acting Hydraulic 0.19 Electrical 2.62 Single acting 2 stage multi vessel Hydraulic 0.2 Electrical 1.26	Single acting 3 stage system was manually actuated so the only power consumptions was the pumps being used	[23]

Type of system	Type of study (theoretical or experimental)	Focus of study	Feed water (ppm)	Recovery range (%)	SEC (kWh/m^3)	Notes	Reference
Batch RO atmospheric feed tank, pressure exchange energy recovery device	Theoretical	Analyse the theoretical losses in a batch RO system for seawater desalination	Seawater 35,000ppm	Using ROSA 49.8% using model developed in this paper 49.2	2.06	The SWRO system designed in this paper was not fabricated	[8]
Batch and semi-batch RO	Theoretical	Review of all low carbon emission desalination methods	Seawater 35,000ppm	50%	1.6	This paper details many other desalination processes. This is just for the batch and semi-batch predictions	[24]
Free piston solar thermal batch RO	Experimental and theoretical	Reviewing the energy savings of batch RO in comparison to other RO methods, additionally designing, building and testing a Batch RO solar thermal system	Brackish 3,500ppm	66%	Theoretically 0.17	An experimental SEC was not gathered through this testing	[5]
Free piston solar thermal batch RO	Experimental and theoretical	Designing and testing a solar thermal batch RO system. Testing the experimental and theoretical performance	Brackish 3,000–5,000 ppm Seawater 31,000–45,000 ppm	Experimental BWRO 50% Theoretical BWRO 60–75% Experimental SWRO 18%–20% Theoretical SWRO 15%–50%	BWRO 0.7–1 SWRO 2–3		[25]
Double acting free piston batch RO	Theoretical	Designing a batch RO system that can continuously produce permeate	Brackish 1,000–5,000 ppm	70%–80%	SEC not stated, however a target energy consumption of 0.25 kW was stated	The paper states the system was in construction	[7]
Single acting free moving piston batch RO	Theoretical	Optimising the design of a batch RO system	Brackish	80%	<0.4	The paper is used to design a system that is currently being implemented at the University of Birmingham	[11]

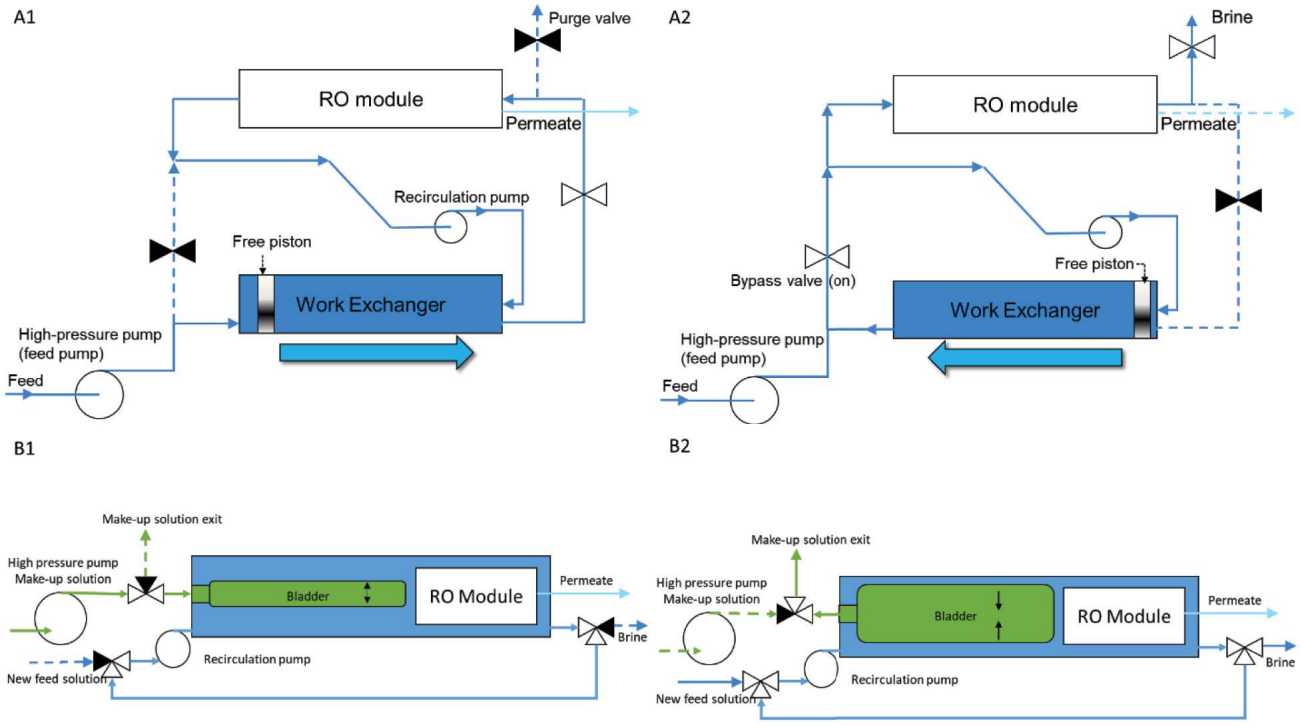

Fig. 1. (A1,A2) show the free moving piston design developed by Park et al. [11] and (B1,B2) show the bladder design developed by Wei et al. [10]. A1 shows the free moving piston design in the pressurisation stage; here the piston is forced to the right-hand side where the batch of saline water is pressurised, permeate passes through the membrane and the concentrate is recirculated back into the batch via the recirculation pump. When the free piston reaches the right-hand side of the vessel the purge and refile phase are activated (A2). During the purge and refill stage the piston is forced to back to the left-hand side of the vessel, a new saline feed fills the right-hand side of the work exchange vessel and simultaneously flushes the rest of the system. Similarly, in (B1) this is the pressurisation stage of the bladder system, a make-up solution is forced into the bladder causing the bladder to expand and pressurise the batch of saline water within the pressure vessel, this forces permeate through the membrane and the concentrate is recirculated back into the batch. When the bladder is fully expanded no more pressure can be added so the purge and refill (B2) stage is triggered. During this stage the high-pressure pump is switched off and the bladder is vented to atmospheric pressure the make-up solution can be recirculated to be used in the next pressurisation cycle, the recirculation pump is used to supply a new feed of water as well as flushing the membrane.

der Waals, Lewis acid-base, and electrostatic double layer forces and ligand-receptor bonds between the micro-organism and polarized bonds, charged groups or OH groups in the conditioned surface [41]. The micro-organisms usually attached to the membrane in points of turbulence, like downstream of the feed spacer layers, due to the lack of flow [30,40]. Once a micro-organism has become trapped in the feed spacer channel, it will remain there until the flow characteristics change. Many factors can affect the attachment of the microorganisms, such as membrane characteristics, flow characteristics, feed nutrient concentration, feed solution micro-organism concentration [30,38,40,41].

3.1.2. Growth

Once attached, further micro-organisms are brought to the activation site by the feed water. The feed water also supplies nutrients to the membrane, which nourish the micro-organisms causing lateral growth across the membrane. Once the biofilm is formed it will disrupt the function of the feed spacer within the membrane element resulting in an increased concentration polarisation, which will lead to more salt passing through to the permeate. Additionally, the biofilm will cause an increase in operating pressure and overall energy consumption of the system [42–44].

Organic fouling by macro molecules will be explained under colloidal fouling in section 3.3.

3.2. Inorganic scaling

Inorganic fouling by scaling is caused by precipitation of sparingly soluble salts. This process can occur by two mechanisms: the formation of salt crystals in the bulk solution, known as homogenous crystallisation; and heterogenous crystallisation, that is, the formation of salt crystals on the surface of the membrane or a suspended solid in the bulk solution [34,35,45]. Both mechanisms are dependent on the degree of saturation and on how long the fluid remains at a supersaturated state [46].

Many factors determine the mechanism of scaling. Firstly, at lower supersaturation indexes (SI), heterogenous crystallisation is more common; whereas at higher

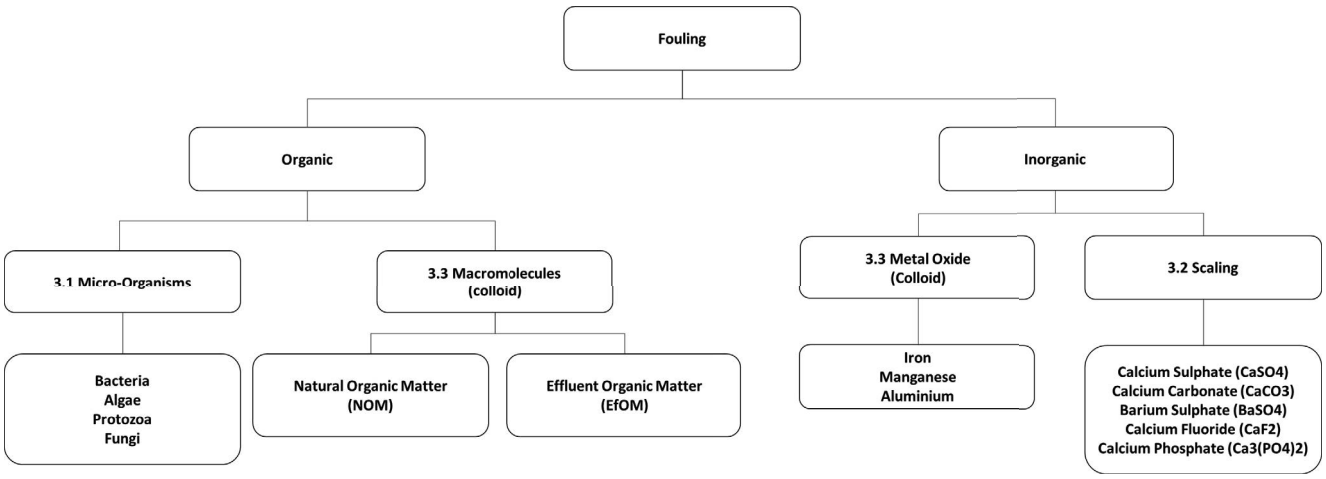

Fig. 2. Categories of fouling that will be reviewed in this study. Fouling can be broken down according to the two main types of foulant, organic and inorganic. The diagram also shows 3 mechanisms of fouling (micro-organism, scaling, colloidal).

SI values homogenous saturation becomes more common [35,47]. Secondly, temperature is an important factor. In a study on organic and inorganic fouling in nanofiltration, Her et al. [48] found that common salts, such as calcium carbonate and calcium sulphate, formed small crystals in the bulk solution that stacked on the membrane surface at 20°C–30°C (homogenous nucleation). However, when running the same experiment at lower temperatures (10°C–20°C), they observed lateral growth of surface crystals (heterogeneous nucleation).

The pH also influences the mechanism of scaling. Lowering of pH disfavours transformation of bicarbonate to carbonate, thus reducing carbonate scaling [49]. The hydrodynamics of the system also play a role in determining the fouling mechanism. A study by Oh et al. [50] focused on developing a model for scaling of various RO arrangements. They found that high cross flow velocity and low rejection favoured bulk crystallisation, while opposite conditions favoured heterogenous crystallisation [50].

Another factor that influences scaling is the presence of organic foulants. Quay et al. [51] studied the relationship between inorganic and organic fouling, using silica as the inorganic compound and a combination of bovine serum albumin (BSA) and lysozyme (LYZ) as the organic compound. It was found that, in solutions where the silica and the proteins were present, there was a faster flux decline when both fouling phenomena (organic and inorganic) were simulated.

Both crystal formation mechanisms follow the same three-stage process of supersaturation, nucleation and growth. Each stage is now reviewed separately:

3.2.1. Supersaturation

Below the supersaturation level, a solution is in a dynamic equilibrium, where opposite charged ions collide and separate. However, at higher concentrations the ions can create activation sites for crystals to form, this is when the fluid is said to be supersaturated [45]. The point of supersaturation can be expressed by the activity of the ions making up the salt and the solubility product [46]:

$$\left[\frac{\mathrm{IAP}}{K_{\mathrm{sp}}}\right] \tag{1}$$

where SI is the saturation index; IAP is the ion activity product, the product of the activity coefficient and the concentration factor of each ion in the salt; K_{sp} is the solubility product. This is the equilibrium for at which a solid substance dissolves into an aqueous solution.

In a solid salt the activity coefficient is =1, so the IAP is a product of the molar concentration of the salts present in the solid [35,52].

$$\mathrm{IAP} = \left[A\right]_m \times \left[B\right]_n \tag{2}$$

The concentration of each salt ion can be calculated using the concentration factor (CF). The concentration factor is equal to the concentration of the concentrate (C_c) divided by the concentration of feed solution (C_f). Additionally, CF can be calculated using the recovery ratio (R) and the rejection (F) of the membrane:

$$\mathrm{CF} = \frac{C_c}{C_f} \tag{3}$$

$$\mathrm{CF} = \frac{1-\left(R\times\left(1-F\right)\right)}{1-R} \tag{4}$$

The K_{sp} can be calculated by multiplying the molar concentrations of each dissociated ion. In this product, each molar concentration must be raised to a power according to the number of ions present in the formula for the salt. The following shows an example of K_{sp} calculation for calcium phosphate ($Ca_3PO_4^2$):

$$Ca_3(PO_4)_2 \rightleftharpoons 3Ca^{2+} + 2PO_4^{3-} \quad (5)$$

$$K_{sp} = [Ca]^3[PO_4]^2 \quad (6)$$

IAP < K_{sp} – Precipitation is avoided; IAP = K_{sp} – Solution is saturated (threshold of precipitation); IAP > K_{sp} – Supersaturated solution – precipitation will take place until IAP = K_{sp} [35,46].

3.2.2. Nucleation

Nucleation is the first stage after supersaturation, whereby ions form a new phase. Dissolved solids form crystalline lattice structures, most of which will re-dissolve into the bulk solution. However, if the nuclei are large enough the crystal will become stable. This can take place via the two routes of heterogenous or homogenous crystallisation. Homogeneous crystallisation dominates at higher supersaturation levels [28,35,46,52].

Homogenous nucleation theory developed by Söhnel and Nielsen in 1971 formed the basis for most modern nucleation theories [45,53]. Heterogenous nucleation models were derived from these by adjusting two variables, the contact angle and the interfacial tension [54]. These two variables are the contact angle and the interfacial tension [54]. In homogenous theory the contact angle is 1, however due to additional surfaces present in heterogenous nucleation this contact angle typically decreases which promotes nucleation [29]. Additional foreign bodies in the solution effect the interfacial tension which plays a role in the heterogenous nucleation rate [29].

Nucleation rates are dependent on supersaturation levels. As the supersaturation index increases, the critical nuclei size required to form a stable crystal reduces [45,55]. In addition, the temperature affects the nucleation rate, as temperature increases the nucleation rate does too [35]. Heterogeneous crystal formation can be dependent on other foulants and foreign bodies in the solution. In homogenous theory, the angle of incidence between nuclei collisions has an impact on formation of crystals [51]. Impurities in the water can reduce this, creating an easier surface for nuclei to adsorb to which reduces the induction time of crystal formation [29].

3.2.3. Growth

There are two main growth stages in inorganic scaling:

- *Growth around the nuclei.* As the nuclei becomes stable, they start to attract other ionic pairs, these form micro-crystals, which then combine with other micro-crystals in the solution which form macro-crystals. Macro-crystals have the tendency to adsorb to membrane surfaces, which leads to the next stage of growth [29].
- *Macro-crystal growth on membrane surface.* This is the growth of the foulant layer on the membrane surface. After the crystal attaches to the membrane surface, the macro-crystals grow laterally to more activation sites and cover more surface area [29,35].

Inorganic fouling by metal oxides is discussed next.

3.3. Colloidal fouling – macromolecules and rigid inorganic matter

Colloids are defined as fine particles with dimensions of 1–1,000 nm. These particles are too big to be removed by diffusion, and too small to be removed by shear forces on the membrane surface [56]. Attachment of colloids to the membrane surface is described by the Derjaguin-Landau-Verwey-Overbeek (DVLO) theory. This theory states that the colloid-colloid interactions are a sum of the van der Waals forces, and that the colloid-membrane surface interaction is governed by electrostatic interaction forces [57,58]. Once attached, these colloids block the membrane surface, causing flux decline and pressure increase [59]. Colloids are classified as two types [59–61]: rigid inorganic matter and organic macromolecules [56]. Rigid inorganic matter includes particles such as silica/silicate, a range of metal oxides such as aluminium oxide, manganese oxide and elemental sulphur/metal sulphides. These are typically found in groundwater sources.

Organic macromolecules are larger organic molecules present in a range of sources. Natural organic molecules, such as proteins/transparent exopolymer particles (TEP), can be found in seawater and groundwater sources [62], while effluent organic matter in the form of humic acids is typically found in water reclamation processes [31].

This section aimed to review literature available on the types of fouling and how and why they may occur. As the review shows, many factors in the RO process can affect the type of fouling that will be present. This makes fouling difficult to predict and is the reason why there is constant research into fouling types and mechanisms. The next section of this review aims to analyse common methods used to detect the type of foulant present during the RO process.

4. Fouling detection methods

4.1. Flux decline

Decline in flux has been a method of fouling detection since the late 1970's. Early theories to interpret flux decline focused on macromolecular fouling through physical mechanisms such as cake layer formations/pore blockage and osmotic pressure changes [63–65].

Constant flux indicates no fouling; whereas a decline in flux shows that fouling has taken place. However, this method is not sensitive enough to detect early stages of fouling, as once flux decreases, fouling is already under way [27]. This is due to the nature of cross flow membranes. Most scaling will start in the downstream area of the membrane where the concentration polarisation is at its highest, then spread upstream. However, the flux decline is not measured locally on the membrane, instead it is an average of the total flux decline, meaning a large proportion of the membrane will be fouled before the flux decline is detected [47].

This theory was put into practice by Gilron and Hasson [66], in an experimental study where the flux decline caused by calcium sulphate fouling was analysed at all points of the membrane surface by using the experimental set up shown in Fig. 3. A flat sheet membrane flow cell with permeate ports evenly distributed across the length of the membrane.

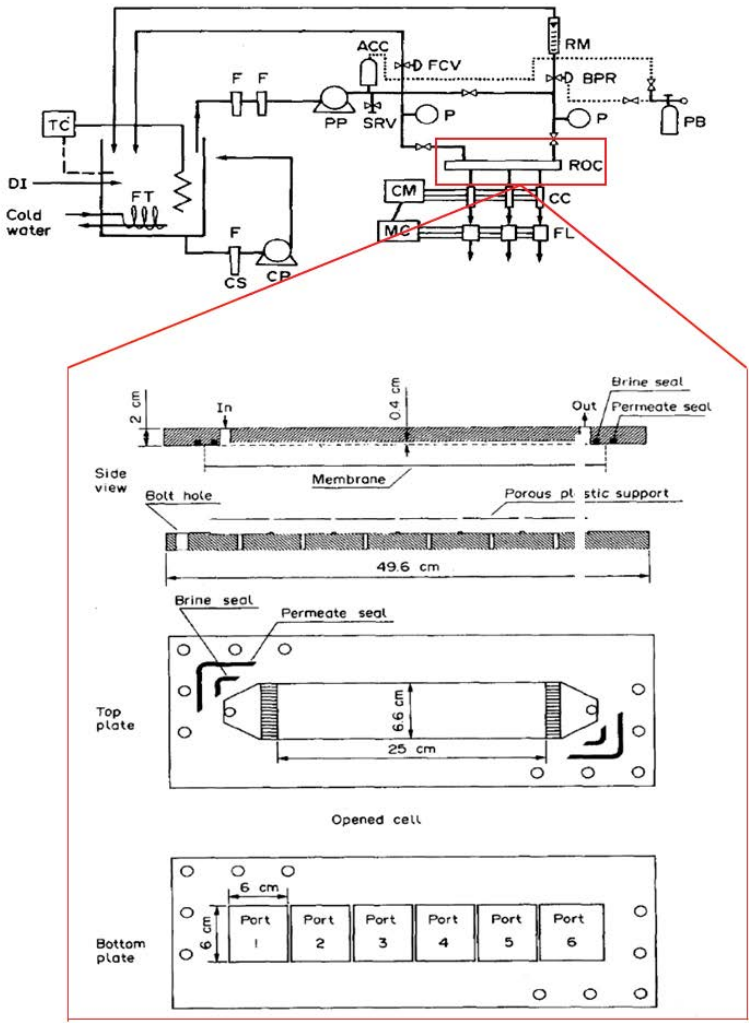

Fig. 3. Experimental set up created by Gilron and Hasson [66] for detecting the flux decline across the length of the membrane. The rig consists of a feed tank with temperature control and recirculation to maintain saturation of calcium sulphate. This saturated solution is then pressured across the flat sheet membrane the flow and pressure is regulated using control valves. The permeate flows through one of the 6 ports across the membrane surface. The permeate from each port is measured allowing a localised flux decline to be detected. The membrane scale coverage was calculated using scanning electron microscopy (SEM) images and using resin moulds of the membrane surface. The results displayed that there was a clear linear relationship between the blockage of the membrane surface area and the flux decline of a RO membrane. This finding contrasted with an earlier theory that attributed flux decline to increase in the cake layer thickness and allowed a model to be produced to predict the flux decline [64].

4.2. In-situ membrane monitoring

Vast amounts of research have been conducted into methods of non-destructive in-situ membrane monitoring devices. In the late 90s, Flemming et al. [67] produced three prototype methods of non-destructive membrane imaging systems, firstly using a fibre optical device, secondly using a differential turbidity device and finally using a Fourier-transform infrared spectroscopy (FTIR) flow cell. The first two methods (Fibre optical and Turbidity device) allow physical particulates to be detected, but provide no way of identifying the particulate substance. These methods can also be influenced by other contaminants in the feedwater which can make the results unreliable. The FTIR flow cell addresses this problem to some extent; however, it cannot be operated as a real time analysis method as the flow cell has to be disconnected from the desalination unit and connected to a FTIR spectrometer.

These methods were developed to produce direct visual observation (DVO) methods, involving using high magnification lenses with cameras to directly observe the cake layer build up and particulate movement across the membrane surface. These processes require a custom transparent module to house the membranes. Methods such as direct observation through membranes (DOTM) have also been developed. These use specially developed membranes which have straight-through pores which, when wetted, become transparent, thus allowing a camera to be mounted on the permeate side of the membrane and view through the

membrane. Nonetheless, this process only allows the first layer of foulants to be observed [68–71].

The next stage of development for membrane monitoring was to produce a method of visualising the membrane surface without need of substantial modification to the standard components. According to Ngene [68], monitoring is valid if the following criteria are met: (1) the device must be representative of a spiral wound membrane, (2) all data obtained from the device must be repeatable to generate a database of results and (3) the device must be able to monitor operational parameters and visually inspect the surface itself [72]. These criteria led to the first prototype of an ex-situ membrane monitoring device known as the flat sheet monitor (FSM). This consisted of a sheet membrane with the same physical characteristics of a spiral wound membrane enclosed between a steel frame with a Perspex visual window, allowing the pressure drop across the membrane to be detected. Thanks to the clear Perspex lid, the membrane surface could be observed using a high magnification camera. However, these devices were large and heavy making them somewhat impractical. A study by Vrouwenvelder et al. [73] focused on developing a smaller scale membrane monitoring device known as the membrane fouling simulator (MFS) as shown in Fig. 4.

These MFS devices are a similar construction to FSM but a fraction of the size. An initial FSM measures 0.32 m × 1.03 m × 0.07 m with an effective membrane length of 0.9 m whereas the MFS measures only 0.07 m × 0.30 m × 0.04 m with an effective membrane of 0.20 m × 0.04 m. This reduction in size requires less water and chemicals to be used in experiments. Various studies by Vrouwenvelder et al. [73,75–77] have shown that the MFS devices are accurate in representing a spiral wound membrane and capable of detecting early signs of fouling. These devices are typically installed downstream of the tail RO element and simulate the conditions in that element.

There are currently no studies to the authors' knowledge that specifically focus on the integration of a membrane monitoring device in-situ with batch RO. However, a recent study by Sarker and Bilton [78] focussed on the real-time computational imaging of scale formation under intermittent RO operation. The intermittent process was similar to the batch RO process, in the sense that the high pressure was released between cycles and that the salinity of the feed was reduced periodically. Sarker and Bilton [78] used a small plate-and-frame imaging device that allowed a sample of the membrane to be viewed. Contrary to expectation [79,80], they observed that intermittent operation actually reduced the scale formation and the formations were more uniform in shape, suggesting that the osmotic backwashing, which occurs when the pressure is released, also has a positive effect on mitigating the scale formation [12,78].

4.3. Membrane autopsy

Membrane autopsies are common methods used in industrial systems to determine the foulants present. As the name suggests, the procedure takes place once the membrane has become badly fouled and is no longer in use. Many tools can be used during the autopsy to allow analysis of the foulants. These tools include, but are not exclusive to, visual observation (VO), laser ionisation mass analysis (LIMA), salt density index, X-ray fluorescence (XRF), and scanning electron microscopy (SEM) [81]. Each tool has can detect different types of foulants. Butt et al. [82] used a range of these tools to identify the foulants present on membranes that were used in pilot experiment which utilised RO unit with an antiscalant dosing unit. The system was fed with brackish groundwater with a high CO_3^{2-} and SO_4^{2-} scale potential and was therefore limited to a 70% recovery so the brine was below the saturation level of silica scaling. The XRF identified large amounts of calcium and magnesium phosphates and the SEM identified that most of the foulant layer was amorphous [82]. In a more recent study by Fortunato et al. [83], the effects of pre-treatment on seawater RO were analysed using a membrane autopsy of a fouled membrane using the following tools: liquid chromatography with organic caron detection (LC-OCD), inductively coupled plasma mass spectrometry (ICP-MS), scanning electron microscopy with energy dispersive spectroscopy (SEM-EDS), total suspended solids (TSS) and adenosine triphosphate (ATP). The SEM-EDS and

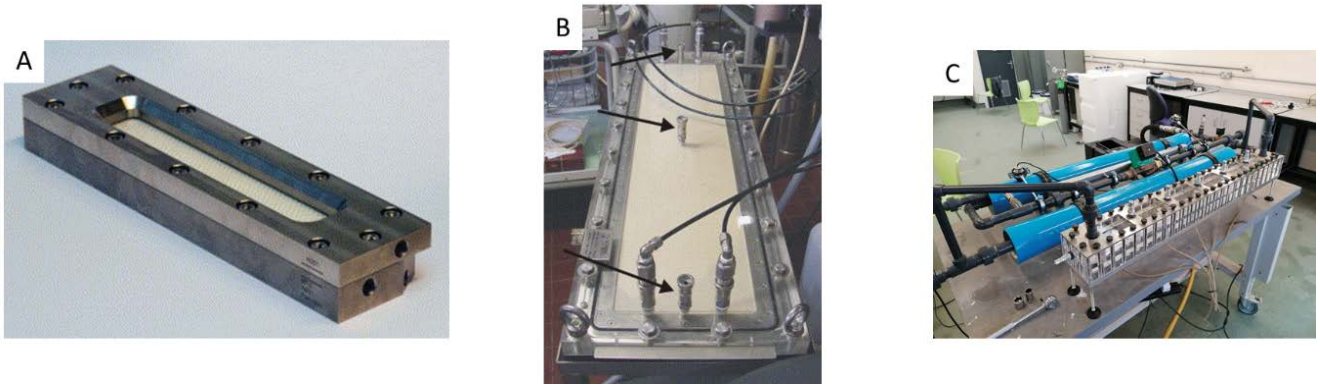

Fig. 4. Shows 3 examples of membrane fouling simulators, (A) being a small compact simulator that allowed for a lower dosage of chemicals to be used when running experiments [73], (B) was an early development by Vrouwenvelder et al. [73] and (C) is a simulator developed by the authors based on a design by Siebdrath et al. [74] this system aimed to replicate the exact flow characteristics within the spiral wound membrane over the full length of a typical membrane.

ICP-MS methods identified a range of inorganic deposits such as aluminium, iron and magnesium silicate, while the LC-OCD process was used to identify the composition of the organic foulants.

4.4. Ultrasound time domain reflectometry (UTDR)

A UTDR set up typically consist of a transducer, receiver and a contact medium – in this case comprising the water, foulant and membrane surface [27]. Differences in acoustic property cause the wave to be partially reflected at each interface (e.g., the water-fouling interface), such that the time taken for the wave to return measures the thickness of each layer. UTDR is commonly used to detect salt crystal formation and colloidal foulants, as their acoustic impedance differs substantially to that of water. Most biofilm layers consist mainly of water, which means they have a very similar acoustic impedance to that of water which makes it difficult to detect the layer structure [84,85]. UTDR has been found to be a reliable non-invasive method of identifying early stages of crystal formation and organic-colloidal fouling. It cannot, however, be used to identify the chemical nature of foulant layer which is a big drawback when attempting to use UTDR as method of optimising the membrane RO process [86,87].

4.5. Longitudinal pressure-drop

During the RO process, two types of pressure drop can be seen: the transmembrane pressure drop (TMΔP) and the longitudinal pressure drop (LΔP) as shown in Fig. 5 [67,88]. A fouling-detection method commonly used in RO plants involves monitoring the increase in the longitudinal pressure drop, while the flow characteristics (i.e., feed pressure and flow rate) within the system are kept consistent. Such increase tends to indicate fouling of the feed spacer. Typically, biofouling occurs near the inlet of the membrane element whereas scaling occurs near the exit [3,27,37,67].

As well as being used to visualise membranes, MFS can be used to detect pressure drop along the length of a membrane [72,73,75–77,89]. The effects of linear fluid velocity on membrane pressure drop was studied by Siebdrath et al. [74]. A MFS was used to detect the pressure drop over 1m of membrane. It was found that an unfouled membrane gave a pressure drop from 0.1 to 1.75 bar at a linear flow velocity from 0.1 to 0.6 ms^{-1}. In the presence of biofouling, pressure drop increased from 0.2–2 bar over a period of 6 d at a fixed velocity. The longitudinal pressure drop was measured in a separate study by Vrouwenvelder et al. [77] to determine what effect the feed spacer has on the biofouling process. Membranes with a feed spacer present experienced an increased pressure drop of 120 mbar.

Typical pressure drop increases in these biofouling experiments varied from 40–250 mbar (10%–50% increase) depending on the fluid velocity, feed pressure, temperature and feed spacer designs [72–75,77,90]. In large scale plants, a cleaning process will take place once the longitudinal pressure drop has increased by 10%–15% [38,68,91].

5. Typical fouling mitigation methods

All RO plants use pre-treatment methods to remove foulants from the feed water and to prolong the life of the RO membrane, the pre-treatment methods can range from chemical methods such as antiscalant-dosing to physical methods such as membrane filtration [92]. Fig. 6 shows an overview of the main pre-treatment methods. Further processes will be described in this section.

In industrial RO plants, the pre-treatment process typically comprises settlement/screening to remove larger suspended solids, coagulation to remove smaller solids and most organic foulants, followed by media filtration. Chemical dosing can also be performed along the way.

5.1. Physical pre-treatment

5.1.1. Settlement tanks

Settlement tanks or ponds can be used to remove large suspended solids (>1 mm) in the feed water such as gravel and sand. This method uses a natural separation processes where heavier particles naturally settle to the bottom of the tank. This method relies on a settling time. For silt particles, settling time is in the region of 3 h, making it a practical solution. However, for smaller colloidal particles the settling time could be in excess of 3 years [92,93].

5.1.2. Coagulation

Once the large, suspended solids have been removed, the next stage is to remove smaller suspended solids. This is achieved via coagulation. Coagulation is the processes of adding chemicals to the water to cause an amalgamation of particles in the stream, which can then be removed by flocculation [94,95]. The most common coagulants are either

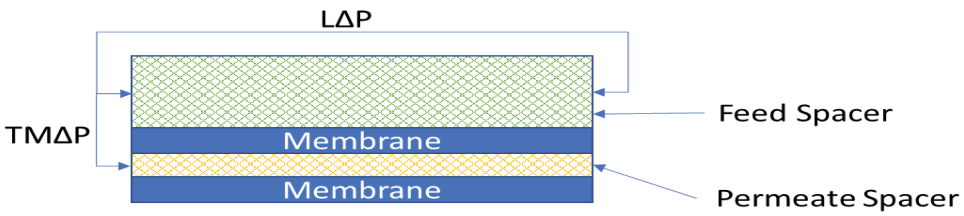

Fig. 5. Diagram displaying the two types of pressure drop experienced during the RO process, the transmembrane pressure drop is the pressure drop from the feed side to the permeate side of the membrane. The longitudinal pressure drop is the pressure drop between the feed in and brine out of the membrane.

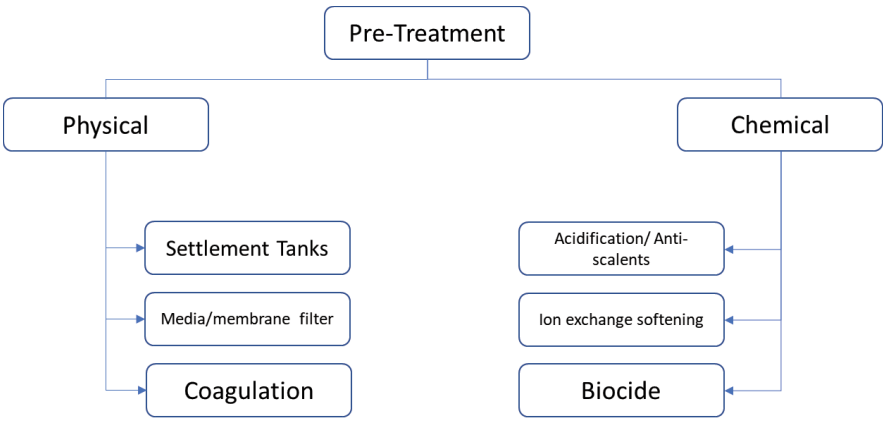

Fig. 6. Classification of pre-treatment methods.

iron-based (ferric chloride and ferric sulphate) or aluminium-based (alum and aluminium chloride) [94,96,97].

The suspended solids present are usually negatively charged, while the added metal salts precipitate and form positively charged metal hydroxide particles. These particles can then remove suspended solids form the water via a precipitation process or an adsorption process. The choice of process depends on the physiochemical make-up of the water [94,96,98,99].

The type of feedwater can play a role in selection of coagulant used. For feedwater with a typically lower pH, such as ground water, alum-based coagulants can be used. Alum-based coagulants are still insoluble at lower pH values. However, in the case of seawater desalination, where the raw feed has a pH typically higher than 8, the alum-based coagulants will become highly soluble and may cause problems downstream [94].

Iron-based coagulants have proven to be better in reducing dissolved organic carbon (DOC), colour and increasing the ultraviolet transmittance than the aluminium-based counterparts, over a range of pH values and dosage quantities [97]. In addition, ferric chloride is relatively insoluble meaning that minimal Fe will be present after the pre-treatment process, thus avoiding and precipitative scaling in processes downstream [94]. For these reasons, iron-based coagulants are usually preferred in seawater desalination.

5.1.3. Media/membrane filtration

A common practice is to use a media filter upstream of a membrane filtration process. Many plants, however, use only media filters. Media filters can have multiple layers depending on the design of the system and the feed water quality. The feed stream is passes downward through the media filter, in which each layer has a progressively smaller pore size to remove smaller particles. Common media to include sand, anthracite, carbon and garnet [100]. Specially for removing biological matter from the water biological activated carbon reactors (BAC), rapid sand filtration (RSF) and slow sand filtration (SSF) can be used [101–103].

Initially the only pre-treatment method using membrane filtration was microfiltration (pore sizes between 100–5000 nm); however, further research has gone into the use of finer membranes (nanofiltration (NF) and ultrafiltration (UF)) [104–112]. The consensus from these studies is that having NF/UF pre-treatment will; allow for higher designed flux and recovery of the RO system, less regular replacements of the RO membrane, less chemicals needed in the pre-treatment process and the capital cost of these methods are generally more than the more conventional methods. These positive findings have led to finer membrane pre-treatment processes being adopted into industrial use [105].

SSF is one of the oldest water treatment methods. It typically runs continuously with minimal cleaning procedures. Sand filters have particles 0.1–0.35 mm in diameter and have relatively low hydraulic load resulting in contact times of 3–12 h. Due to the small particle size and large contact time, the effluent of the SSF tends to have a low turbidity and may not require a previous coagulation step [113].

The long-term performance of SSF as a means of controlling biofouling in a seawater RO system was studied by Oliveira and Schneider [114], who found that after the initial filter maturation period (2–3 months) the microbial growth potential reduced by 90%. SSF has an advantage over other membrane pre-treatment such as NF/UF, in that SSF systems are comparatively simple in design and do not require periodic replacement like membranes. A disadvantage of SSF, however, is the large footprint associated with the low hydraulic loading [115]. Scientific advances have been made in SSF to increase the hydraulic load. This led to development of RSF systems which typically have a flow rate 300 times that of SSF [113]. RSF systems are widely used in most seawater reverse osmosis (SWRO) plants globally due to their cost and effectiveness at removing particulates greater than 0.35 mm. Unlike SSF, RSF is not effective at removing biofouling contaminants, so require some form of coagulation process prior as well as needing regular backwashing [102,113]. However, a study by Bar-Zeev et al. [102] has shown the potential of RSF for removing some bio contaminants with adequate system design and bed maturation.

In a comparison between SSF and MF pre-treatment for inland RO, Corral et al. [116], found that MF was significantly better at reducing membrane fouling. They also found MF to be cheaper at \$0.21/m^3 compared to \$0.25/m^3 for SSF. For continued use, SSF would require more regular

cleaning processes which could further increase the cost of operation; however, it was recently discovered that in a SSF all beneficial effects were experienced in just the first 30 cm of the filter, meaning the depth of the SSF can be drastically reduced compared to common designs (insert depth), this discovery could significantly reduce the cost of SSF making SSF a more viable option of pre-treatment [114].

5.1.4. Ultraviolet (UV) radiation

UV pre-treatment is a process where the feed water is exposed to UV radiation which alters the physico-chemical and biological characteristics of natural organic matter within the feed water, ultimately killing microorganisms [117]. UV can be used as an alternative to biocides and oxidants [118]. Typically, there are two types of UV lamps used low pressure (LP) and medium pressure (MP) [119–121]. LP lamps tend to produce radiation at wavelengths of approximately 250 nm and are used for controlling microorganisms, whereas MP lamps tend to have a shorter wavelength (185 nm) and are used to control the total organic carbons in the water [119,120].

It was found that LP lamps were able to reduce active bacteria counts by a factor of 2, as determined in an experiment performed by Di Martino Patrick et al. [122] where two simultaneous NF systems were operated with the same feed water, one with pre-treated by a LP UV lamp. The UV-treated feed water showed no change in dissolved organic carbons and biodegradable organic carbon, but it did show a reduction in active bacteria.

The effects of UV as a means of pre-treatment for ultrapure water production via RO were investigated by Jin et al. [118] who found that UV pre-treatment, though effective at removing biofoulants, increased the chances of silica fouling due to the UV's effect on aggregating colloidal particles which potentially can form a cake layer on the membrane surface.

5.2. Chemical pre-treatment

5.2.1. Acidification/antiscalant

Acidification is the process of adding an acid solution to the feed water to reduce the pH. It is used to reduce calcium carbonate scale formation. Common acids used are hydrochloric and sulphuric acid, the latter being more common and can be used at a wider range of concentrations between (20%–90%), whereas hydrochloric acid is typically used at concentrations <40%. Both acids have drawbacks [123]. Sulphuric acid increases the concentration of sulphate ions in the feed solution which can increase the chances of sulphate fouling; and the hydrochloric acid increases the concentration of chloride ions which are less effectively rejected by RO membranes than sulphate ions [35].

Acid dosing is a cheap and effective method of removing $CaCO_3$ scaling but does have downsides. For example, commercially available acids tend to be contaminated with some form of metals which can encourage other mechanisms of fouling. Because of these secondary effects, most industrial systems opt for dosing of antiscalants. Antiscalants have been in use since the latter half of the 20th Century. The first commercially used antiscalants were sodium hexametaphosphate, an inexpensive antiscalant that is still used in some plants today. However, more modern polymeric organic scale inhibitors are more stable and are more effective than sodium hexametaphosphate [124]. Scale inhibitors function by three different mechanisms:

- *Threshold effect*: This prevents the early stages of crystal formation. Using a sufficiently large dose of antiscalant, soluble salts that have exceeded their solubility limits will not precipitate.
- *Crystal distortion effect* is where the inhibitor affects the structure of the crystal formation. The crystals become irregular in shape, creating a poor surface for other crystals to attach.
- *Dispersancy effect*: The scale inhibitor causes a surface charge in the crystals which causes the crystals to repel each other [124,125].

Developments have been made in novel scale inhibitors. A study by Li et al. [126] compared the performance of a newly developed non-phosphorous copolymer to readily available scale inhibitors, Flocon-135 and Flocon-100, on the inhibition $CaSO_4$. It was found that the new novel inhibitor was cheaper, more effective over a wider range of pH, required a smaller dosage, withstood higher supersaturation limits and was less affected by iron ions [126]. Additionally, a study by Shahid et al. [127] reviewed the performance of CO_2 as a scale inhibitor. The idea of using CO_2 as a scale inhibitor follows the same method as acidification, that is, the CO_2 will reduce the pH of the feed stream which will reduce the chances of inorganic scale formation. The performance of CO_2 was compared to a readily available anticalants to show that the CO_2 performed adequately and was less than half the cost of commercial antiscalant. However, CO_2 is only capable of removing $CaCO_3$ from the solution, meaning that a CO_2 injection process will need to be used in combination with another pre-treatment method [127].

5.2.2. Ion exchange softening

The aim of this pre-treatment process is to remove scaling ions such as Ca^{2+} and Mg^{2+}. This is important for gypsum ($CaSO_4{\cdot}2H_2O$) which is not sensitive to pH therefor cannot be solubilised by acidification as stated previously. Ion exchange systems are typically situated at the last stage of the pre-treatment process, where feed water with high Ca^{2+} and Mg^{2+} level is passed through a column of resin material selected for its ability to attract the positive ions to its surface [128]. Vermeulen et al. [129–131] studied a novel process of using the brine from the RO system as the ion exchange medium. To make this a viable process, however, additional salts needed to be added to the brine. This process utilises an ion exchange unit with a cation exchanger that allows the Ca^{2+} and Mg^{2+} to be replaced with Na^{+} ions which has a much lower scaling potential than the other cations [129–131]. However, these studies were not seen as a viable solution when they were conducted, due to the low salinity of the brine outlet, poor modelling of ion exchange units and the lack of importance given to brine management during the 1970s when the studies were conducted [129–131].

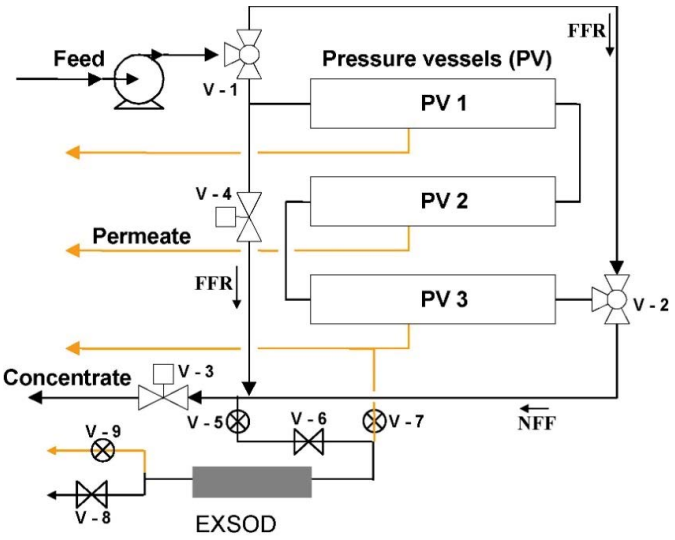

Fig. 7. FFR schematic layout using an EXSOD for flow reversal trigger [164].

In recent years, a study conducted by Venkatesan and Wankat [132] focused on the shortcomings of the earlier research conducted by Vermeulen et al. [129–131]. Since the earlier research, three areas have evolved. Firstly, advances in membrane technology have reduced the need for additional salts to be added to the brine outlet of the modules to regenerate the ion exchange column. Secondly, advances in the modelling and simulation of ion exchange systems have become a lot more accurate, enabling better system design. Finally, brine disposal costs have escalated such that they now account for 80% of the running costs of RO [133].

Only one study could be found that integrates an ion exchange softening process with a semi-batch RO system [134]. This study aimed to investigate which would be more viable as an off-grid desalination system: plug-flow RO or a semi-batch RO, both with an ion exchange pre-treatment stage. The study concluded that the semi-batch RO system allowed for a higher recovery (92%–95%) and less fouling than the plug-flow system (86%).

5.2.3. Biocides and chlorination

Biocides are chemical disinfectants that can be added to the feed solution to prevent the growth of microorganisms. The most common biocides used are free chlorine ($HOCL_2{\cdot}OCL^-$), monochloramine (NH_2Cl), chlorine dioxide (ClO_2) and ozone [135] and a lesser used 2,2-dibromo-3-nitriloproprionamide (DBNPA) [136]. DBNPA is seen as less harmful chemicals for the membrane element [135–137].

The chlorine-based biocides introduce additional chlorine into the feed solution. This is usually achieved by adding chlorine gas or sodium hypochlorite. The issue with the addition of free chlorine is the oxidisation potential and attacking of the polyamide membrane; therefore, at the end of the pre-treatment process, the water must be dechlorinated typically using sodium bisulphite or granular activated carbon [135].

Due to the added complexity of chlorination and dichlorination of the water, advancements were made in non-chlorine based biocides such as DBNPA. The lab based study by Siddiqui et al. [89] found that a continuous small dosage of DBNPA (1 mg/L) was effective at preventing biofouling from forming and higher doses (20 mg/L) on already fouled membranes was shown to prevent the growth of further biofilm and stabilised the pressure drop. These lab results were supported with large scale implementation by Boorsma et al. [138] and Caron et al. [139].

Biocides cannot remove 100% of living bacteria in the feed water and any residual bacteria can attach to the membrane and multiply over time as nutrients reach the membrane. This is why biofouling is the most common form of fouling in RO systems [140]. A downfall of biocides is that they contaminate the brine and must be disposed of in an effective manner. In a study about the environmental impacts of seawater brine disposal, Lattemann and Höpner [141] assessed the impact of left-over pre-treatment chemicals on marine life. The study found that the free and combined chlorine residual from most seawater RO plants greatly exceeded WHO recommendations. This has prompted vast amounts of research into novel pre-treatment methods to reduce chemical residues and disinfection by-products. However, none has been widely accepted as a replacement for chlorine [137,142–149].

Current methods of pre-treatment still have negative effects on the RO process and in many cases can account for a large proportion of the CAPEX of the RO plant. Some advances have been made in using less harsh chemicals, less energy intensive and less wasteful processes however there is still vast room for improvement. This will be expanded on in section 6 in which we review the potential of batch RO to avoid or reduce pre-treatment.

6. Hydrodynamic effects in batch RO

The BRO process is an unsteady desalination process, meaning that the flow over the membrane does not follow the same characteristics as in standard continuous RO systems, such as unidirectional flow, varying salinity and

pressure with time and points of excessive crossflow velocity [9–12]. Due to the unsteady nature of the process, the following flow characteristics have been observed in the BRO operation process. This section aims to summarise each characteristic and relate them to the BRO process specifically. These unusual characteristics are likely to influence fouling. Very few studies have investigated directly the potential benefits of BRO as a method of fouling mitigation, but preliminary data from Wei et al. [22] suggest that the salinity cycling of the batch process reduces the chances of scale formation. In addition, a study conducted by Riley et al. [16] suggests that the semi-batch closed circuit desalination process has a beneficial effect in mitigating biofouling during the reclamation of oil and gas waste streams. The study proved that the effects of fouling were minimal over 440 h of operation.

6.1. Osmotic backwash

Osmotic backwashing is a proposed chemical free cleaning process where water is drawn back through the RO membrane by forward osmosis [150,151]. This has been demonstrated in lab studies where a hypersaline solution has been periodically passed through the feed side of the RO membrane causing permeate to pass back through the membrane and subsequently remove a fouling layer. This was found to remove 70%–79% biovolume, 78% total organic carbon and 66% of proteins from the membrane surface [152].

Preliminary data from prototype testing of batch RO show that some osmotic backwashing is experienced at the start of the purge-and-refill cycle because of the salinity difference across the membrane (supersaturated batch and fresh permeate) [10,19]. This phenomenon was reported in lab studies conducted by Wei et al. [10] on the bladder batch RO system. The osmotic backwash phenomena can be accentuated by using a supersaturated feed solution of a soluble salt (NaCl, Na_2SO_4, $MgSO_4$) causing the backwash process to take place for longer than in normal batch RO. The type of salt and concentration was studied in detail by Dana et al. [151]. It was found that NaCl was a better draw solution for cleaning seawater RO membranes, whereas brackish water RO membranes reacted better to sulphate-based cleaning salts. Another method of forcing osmotic backwash can be achieved by pressurising the permeate line, a spiral wound membrane for accommodating this was invented by Ando et al. [153,154]. This module allowed a back pressure between 0.5–3 bar. This back pressure will allow fresh water to permeate back through the membrane thus having the same effect [153,154].

The use of osmotic backwashing as a cleaning mechanism for organic fouling was first suggested in a study by Spiegler and Macleish [155]. Membrane channels were pressurised up to 41 bar, then reducing to 0.3–2 bar so that osmotic backwash occurred. The system experienced a flux decline of 14.5% in 20 h of operation and the osmotic backwash restored 50% of this decline [155].

Since then, considerable amount of research has been conducted on the ability to remove or reduce the need for chemicals in the cleaning process of RO membranes [156–158]. Further studies were carried out for a range of different feed water types and osmotic backwashing cycle times. In a study by Bar-Zeev and Elimelech [152], the effects of osmotic backwash on removal of biofilm were assessed, with osmotic backwash cycles of between 50–60s at a maintained feed pressure of 13.8 bar. It was found that a 63% reclamation of flux decline was achieved, as well as reducing the volume of biofilm by up to 79% [152].

Similar results were found in a study by Ramon et al. [150] in which the effects of osmotic backwash were compared to the effects of chemical cleaning. This study highlighted the importance of integrating osmotic backwash with an additional cleaning mechanism. The osmotic backwash stage lasted 10 min and was coupled with a physical cleaning method such as recirculating de-ionized water after loosening the biofilm. This was compared with just physical cleaning, chemical cleaning and osmotic backwash without the additional physical cleaning. The flux recovery was 22%, 100%, 83%, respectively, and the osmotic backwash with physical cleaning achieved a 93% flux recovery [150].

This theory was further tested in a study conducted by Yip et al. [159] on the effects of osmotic backwash on natural organic matter fouling in pressure retarded RO. It was found that osmotic backwashing at a normalised rate of 5 l/m^2 (approximately 2% of permeate produced during the cycle) could remove most fouling in the support layer, but was unsuccessful in removing foulants from the active layer of the membrane. The results showed a flux recovery of 61.3% after a quick osmotic backwash cleaning [159].

Besides such studies on organic fouling, studies have been conducted on the ability to remove inorganic scaling. For example, Cai and Schäfer [160] set up a bench top experiment using $CaCO_3$ and $CaSO_4$ as the fouling agent. A small membrane monitoring system was used so the scale formation could be inspected, and it was found that the effectiveness of osmotic backwashing of the membrane in operation was highly dependent on the mechanism of scaling, the scale agent, the membrane properties and general operating conditions. Thus, flux recovery varied over a wide range of 30%–96%. This is due to the nature of the scale formation. The scale loosely forms a cake layer on the membrane surface, when the permeate passes back through the membrane this loose scale is lifted and the concentrate stream flushes it away from the membrane. The results of this experiment were confirmed by visual inspection of the osmotically backwashed membrane in comparison to a virgin membrane [160].

6.2. Feed flow reversal

During the purge and refill cycle, the feed flow direction is reversed, allowing fresh feed water to replace the supersaturated solution near the outlet of the membrane element. Initial studies into the use of feed flow reversal (FFR) for scale removal were conducted by Gilron and Korin [161]. The idea of FFR was to allow for higher recovery ratios of feed solutions of sparingly soluble salts to be achieved without increasing the amount of chemicals needed in the pre-treatment process. This method proposes reversing the feed direction of the saline solution, making the previous tail end module the new lead module. This means that the super concentrated solution that had formed around the tail element will be replaced

with fresh feed solution reversing the axial concentration polarisation, effectively resetting the induction time clock for nucleation of salts on the tail element as well dissolves any salt crystals that may have already formed [162,163]. It was found that FFR every 30 min allowed for a continuous RO system to run at 80% recovery for 18h without any calcium sulphate precipitating on the membrane; whereas in the same conditions continuous RO without FFR experienced scaling within 1.5 h [163].

This phenomenon was visualised in a study by Uchymiak et al. [164], in which a brackish water reverse osmosis plant (BWRO) was operated with a solution of calcium, sodium and chloride ions to encourage gypsum salt crystals to form on the membrane. Three pressure vessels containing 6 elements were placed in series with a membrane monitoring device (EXSOD) downstream of the tail element as shown in Fig. 7. The EXSOD allowed live monitoring of the membrane condition and could be used to trigger the FFR process. The study concluded that FFR was effective at reducing crystal formation; however, the optimisation of the system proved difficult, this is due to difficulties in making the EXSOD replicate the exact conditions of the tail element of the process, which resulted in the feed flow reversal happening either too often or not often enough [164].

In later studies [165,166], another method of scale detection was used to trigger the FFR process. A plate and frame cell was fitted with ultrasonic reflectometry sensors to detect early-stage scale formation, which was proven to be a lot more accurate than visually inspecting crystal formation density on the frame and cell membrane, the ultrasonic reflectometry sensors allowed for early-stage formation to be detected before salt crystals were formed in the RO module.

In a recent study conducted by Tang et al. [167], the application of FFR for nanofiltration (FFR-NF) of industrial wastewater was analysed. The aim of many industries now is to move to zero liquid discharge (ZLD) for which membrane methods have potential for great energy savings compared to traditional thermal methods of concentration. This study provides a model and experimental data for the feasibility of using FFR to allow higher recoveries via membrane technology to somewhere close to near-ZLD, after which the final stage can be a conventional thermal process. The results show that using FFR-NF can be a feasible option as a pre-treatment for further ZLD technologies.

During the standard operation cycle of the free moving piston batch RO system, the feed flow direction is reversed at the end of every pressurisation cycle when the purge-and-refill cycle commences [6,11,20,23]. During this cycle, a pressure can be maintained in the module by an adjustable diaphragm valve (V_c), this will allow a fresh feed solution to pass over the membrane at a set pressure, this process takes place until a conductivity sensor on the outlet of the module (c2) reaches a set level relevant to the supply conductivity (c1) – Fig. 8.

An alternative system was designed and fabricated by Davies et al. [7], coined as the double-acting free moving piston batch RO system. Instead of following a two-stage cycle of pressurisation followed by purge-and-refill, the double acting system entered a second pressurisation cycle which introduced fresh water into the tail end of the membrane module. This essentially reversed the feed flow between every batch. Further work has been conducted by Cordoba et al. [17] on the development of a double acting system BRO system; however, no research has been reported on the potential fouling benefits due to the feed flow reversal in the double-acting system.

6.3. Reduced time under supersaturation and salinity cycling

A common theory for scale formation is based around the induction time (the time taken for a stable crystal to form under supersaturated conditions) of specific salt ions present. This theory assumes that the feed water has no other contaminants, so the induction time is determined by the supersaturation and the temperature which determine factors such as critical nuclei radius, contact angle and crystal geometry [54,168,169].

The induction time of calcium sulphate at a range of supersaturation limits was studied by Alimi et al. [170] who found that the induction time decreased from 9,600 to 60 s over the range of 2.6–11 supersaturation index, in BRO the solution only becomes supersaturated towards the end of the batch cycle (depending on the feed water concentration) therefore the supersaturated solution will only have a small amount of contact time with the membrane before the purge and refill cycle is activated [11]. Another study by Dhakal [35] focused on experimentally proving the predicted induction time of calcium carbonate scaling, with and without anti-scaling dosing at a range of pH values and a range of recoveries. The predicted induction time was proven to be accurate. It was in the region of 47–81 min at recovery of 75% and a pH between 8.06 and 7.98. The induction times in this experiment was determined by a change in pH as this indicates salts have precipitated; however, the solutions used in this experiment contained no other contaminants so were not a true representation of scale formation in RO systems [35,52]. As stated previously, this induction time can be drastically reduced by the addition of other impurities/surfaces in the water, because of the decrease in activation energy required to form stable nuclei [171].

In a recent study by Warsinger et al. [12], the fouling resistance of batch and semi-batch reverse osmosis (SBRO) systems were compared. The study aimed to produce a model for scale prediction in BRO focusing specifically on the salinity cycling process. It has been observed that in all batch and semi-batch RO processes that the residence time is very low in comparison to standard continuous RO systems; the residence time in SBRO and BRO is between minutes and hours as the fluid becomes supersaturated towards the end of the batch before being expelled from the system, whereas the residence time in continuous RO is defined as the time between cleaning processes, which can vary from weeks to months. The constant changing salinity from supersaturated to undersaturated is coined as salinity cycling process, which effectively resets the induction time clock at the start of each cycle – provided that all precipitated salts and supersaturated solution are purged out the system. This essentially allows the system to be exposed to supersaturated solutions for a longer period of time [12]. However, little experimental data have been published to

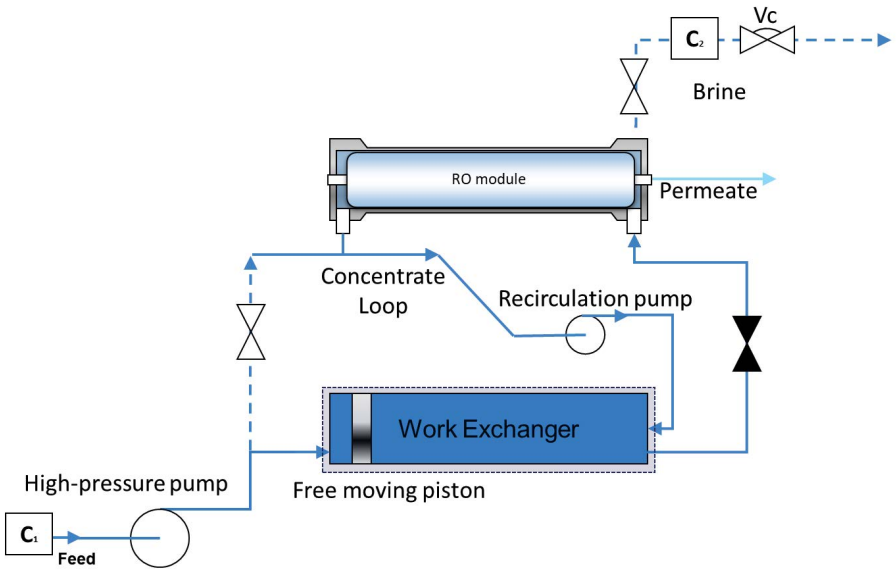

Fig. 8. Schematic diagram of the free moving piston batch RO rig displaying the sensors and valves required to operate with pressurised FFR [11].

validate the claims of this research, and the induction time calculations considered only homogenous crystal formation.

This theory was further expanded in research by Lee et al. [15], where a comparative study of the gypsum scaling propensity of SBRO and steady state RO with partial recycle (SSRO-PR) was conducted. A SBRO and SSRO-PR systems were run with similar operating conditions (recovery ratio and temperature) and the same average feed water characteristics. Scale formation was detected using the membrane monitoring system (EXSOD) as explained in Fig. 4. It was found in the study that SBRO developed scale over a period of cycles, due to inefficient flushing and the scale formation being a stochastic process meaning there is a distribution of induction times. Thus nuclei may form under shorter average induction times than expected [55,162]. In the experiments of this study, the scale formation was detected using the membrane imaging system described earlier in this paper. Due to the method of detection, only fully formed crystal nuclei could be detected. The study suggested that early-stage nuclei are not efficiently washed from the batch during the purge cycle, such that the induction time is not completely reset, thus resulting in scale formation in the SBRO process being more prominent than in the SSRO-PR process. Increased flushing could be used for better removal of nuclei, but at the expense of system recovery [15].

As in the case of FFR, further work is needed in this field to determine whether ideal flushing can be achieved, without sacrificing the performance of the BRO or SBRO system. This may be achieved, for example, by using other detection methods for early-stage nuclei formation such as pH detection (for calcium carbonate scaling) [52]. Alternatively, other BRO and SBRO system designs may reduce the residence time even further. Note that, in the above study, the cycle time ranged from 11 to 20 min [10,19,22], whereas the BRO process proposed by Park et al. [11] has a cycle time of 8–10 min with a flushing cycle of 1–3 min [11], meaning that the membrane is exposed to super saturated solutions for a shorter period.

6.4. Water hammer/pulse flow?

Pulse Flow RO is a method where the feed flow is pulsated. The aim of this method is to allow high flux and high recovery without the addition of chloramine, which results in a chemical free brine [172]. The pulsating flow was patented as a method of cleaning, where the feed flow is pulsated to create a water hammer like effect on the membrane this water hammer effect can effectively remove biofilm already formed on the membrane surface [173,174].

In a study conducted by Liberman et al. [175], the effects of Pulse Flow RO on the reduction of scale and biofouling of membranes were predicted and tested in a 330 d long experiment[1]. The experiment was conducted using a pilot rig installed in California, consisting of one 8″ pressure vessel with seven Dow FILMTEC ECO PRO-400 membranes inside. The feed water used was secondary effluent from a municipal wastewater treatment plant that was treated with a micro filtration process. Additionally, the feed water was pre-treated with anti-scalant to remove the variable of scaling.

The experiment concluded that PFRO removes the need of chloramine as a means of pre-treatment. The pulsating operation (opening and closing the brine valve rapidly) allows a water hammer to be created, which applies a high shearing velocity to the membrane; additionally, the

[1] Total experiment time was 330 d, however the first 130 d were used to optimise the machine performance, and during the last 42 d the 1st and 7th membranes were removed from the rig to be sent for an autopsy and replaced with new membranes.

frequent changes in gauge and osmotic pressure create a less than ideal environment for biofouling to form. The shear velocity required to remove the chance of biofouling is the critical velocity. There is no exact method to calculate the critical shear velocity, but conventional RO systems run at approximately 0.1–0.15 m/s and the PFRO system ejects brine at 1.5 m/s so it can be concluded that the critical velocity is somewhere between this range [175].

The free-piston BRO systems described in studies by Davies et al. [7,23] were designed to operate with a solenoid actuated valve on the brine outlet. It was found that during experimentation the rapid actuation of this solenoid valve was caused a surge in flow velocity across the membrane, however this surge has never been quantified. Additionally, at the end of the purge and refill phase, the solenoid valve was closed suddenly this created a water hammer effect at the start of the pressurisation phase. This shows the possibility of introducing pulsating flushing to the BRO process, which has the potential advantage of further mitigating the fouling process. Further work needs to be conducted on quantifying flow characteristics and the effects they have on the fouling potential of BRO.

As this section shows, much research has been directed to reducing the use of chemicals in the operation of RO systems. Such chemical free/reduced approaches are typically based around specific flow characteristics within the system. In laboratory-based testing these flow characteristics have been found to happen naturally within the BRO process. Further research is needed in the field of BRO to quantify the effects of these flow characteristics on the fouling potential of BRO.

7. Conclusion

BRO is a new emerging method of RO that allows high water recovery as well as low energy consumption. The aim of this paper has been to review recent developments in BRO technology, fouling mechanisms, fouling detection methods and fouling mitigation methods–and finally to describe specific flow characteristics within the BRO process that may have benefits as regards fouling.

A major issue in achieving high recovery is the increased chances of fouling due to the increased concentration of soluble salts and nutrients in the solution. In industrial plants, substantial pre-treatment is used to reduce the chances of fouling. BRO is very promising for off-grid decentralised water treatment where chemicals are hard to source, and where any additional chemicals added to the water may have a negative effect on the surrounding environment – such that chemical pre-treatment methods should be minimised or avoided. It was found in some recent studies on BRO that certain flow characteristics experienced during the standard operation may have a positive effect on the fouling propensity of process. These characteristics have been highlighted to show how and why they occur during the BRO process; therefore, it can be concluded that BRO may reduce the amount of pre-treatment required for desalination.

Lastly, a range of methods has been identified throughout this paper for detecting the type and stage of fouling on the membrane surface. Very few of these are typically used in industrial plants, where simple flux decline and pressure drop are the common methods used to detect fouling. However, once such changes are experienced, it is already too late to avoid the fouling and the system must be switched off for cleaning. Again, this is not ideal for off-grid decentralised applications as it means that essential water supply will be interrupted. In addition, if the fouling is not reversible, then replacement membranes will be needed.

Future developments for this work would be to implement a BRO system with a custom MFS in-situ that allows for the identified flow characteristics to be quantified and ultimately determine whether BRO does have mitigating effects against fouling.

Acknowledgements

LB acknowledges support from the School of Engineering, University of Birmingham, and from the Douglas Bomford Trust.

References

[1] M.A. Shannon, P.W. Bohn, M. Elimelech, J.G. Georgiadis, B.J. Marinas, A.M. Mayes, Science and technology for water purification in the coming decades, Nature, 452 (2008) 301–310.
[2] M. Elimelech, W.A. Phillip, The future of seawater desalination: energy, technology, and the environment, Science, 333 (2011) 712–717.
[3] S.S. Shenvi, A.M. Isloor, A. Ismail, A review on RO membrane technology: developments and challenges, Desalination, 368 (2015) 10–26.
[4] J. Kim, K. Park, D.R. Yang, S. Hong, A comprehensive review of energy consumption of seawater reverse osmosis desalination plants, Appl. Energy, 254 (2019) 113652, doi: 10.1016/j.apenergy.2019.113652.
[5] T. Qiu, Desalination of Brackish Water by a Batch Reverse Osmosis Desalink System for Use with Solar Thermal Energy, Ph.D. Thesis, Aston University, Birmingham, UK, 2014.
[6] T. Qiu, P. Davies, Concentration polarization model of spiral-wound membrane modules with application to batch-mode RO desalination of brackish water, Desalination, 368 (2015) 36–47.
[7] P. Davies, A. Afifi, F. Khatoon, G. Kuldip, S. Javed, S. Khan, Double-Acting Batch-RO System for Desalination of Brackish Water with High Efficiency and High Recovery, Desalination for the Environment–Clean Energy and Water, Rome, 2016.
[8] J. Swaminathan, E.W. Tow, R.L. Stover, Practical aspects of batch RO design for energy-efficient seawater desalination, Desalination, 470 (2019) 114097, doi: 10.1016/j.desal.2019.114097.
[9] D.E.M. Warsinger, J.H. Lienhard, E.W. Tow, R.K. McGovern, G.P. Thiel, Batch Pressure-Driven Membrane Separation with Closed-Flow Loop and Reservoir, United States Patent, US20170239620A1, 2019.
[10] Q.J. Wei, C.I. Tucker, P.J. Wu, A.M. Trueworthy, E.W. Tow, J.H. Lienhard, True Batch Reverse Osmosis Prototype: Model Validation and Energy Savings, The International Desalination Association World Congress on Desalination and Water Reuse, Dubai, 2019.
[11] K. Park, L. Burlace, N. Dhakal, A. Mudgal, N.A. Stewart, P.A. Davies, Design, modelling and optimisation of a batch reverse osmosis (RO) desalination system using a free piston for brackish water treatment, Desalination, 494 (2020) 114625, doi: 10.1016/j.desal.2020.114625.
[12] D.M. Warsinger, E.W. Tow, L.A. Maswadeh, G.B. Connors, J. Swaminathan, J.H. Lienhard, Inorganic fouling mitigation by salinity cycling in batch reverse osmosis, Water Res., 137 (2018) 384–394.
[13] S. Nejati, S.A. Mirbagheri, D.M. Warsinger, M. Fazeli, Biofouling in seawater reverse osmosis (SWRO): impact of module

geometry and mitigation with ultrafiltration, J. Water Process Eng., 29 (2019) 100782, doi: 10.1016/j.jwpe.2019.100782.
[14] A. Efraty, Closed circuit desalination series no-6: conventional RO compared with the conceptually different new closed circuit desalination technology, Desal. Water Treat., 41 (2012) 279–295.
[15] T. Lee, J.Y. Choi, Y. Cohen, Gypsum scaling propensity in semi-batch RO (SBRO) and steady-state RO with partial recycle (SSRO-PR), J. Membr. Sci., 588 (2019) 117106, doi: 10.1016/j.memsci.2019.05.030.
[16] S.M. Riley, D.C. Ahoor, K. Oetjen, T.Y. Cath, Closed circuit desalination of O&G produced water: an evaluation of NF/RO performance and integrity, Desalination, 442 (2018) 51–61.
[17] S. Cordoba, A. Das, J. Leon, J.M. Garcia, D.M. Warsinger, Double-acting batch reverse osmosis configuration for best-in-class efficiency and low downtime, Desalination, 506 (2021) 114959, doi: 10.1016/j.desal.2021.114959.
[18] J.R. Werber, A. Deshmukh, M. Elimelech, Can batch or semi-batch processes save energy in reverse-osmosis desalination?, Desalination, 402 (2017) 109–122.
[19] Q.J. Wei, C.I. Tucker, P.J. Wu, A.M. Trueworthy, E.W. Tow, J.H. Lienhard, Batch Reverse Osmosis: Experimental Results, Model Validation, and Design Implications, AMTA/AWWA Membrane Technology Conference & Exposition, New Orleans, 2019.
[20] P.A. Davies, J. Wayman, C. Alatta, K. Nguyen, J. Orfi, A desalination system with efficiency approaching the theoretical limits, Desal. Water Treat., 57 (2016) 23206–23216.
[21] T. Qiu, P.A. Davies, Comparison of configurations for high-recovery inland desalination systems, Water, 4 (2012) 690–706.
[22] Q.J. Wei, C.I. Tucker, P.J. Wu, A.M. Trueworthy, E.W. Tow, J. Lienhard, Impact of salt retention on true batch reverse osmosis energy consumption: experiments and model validation, Desalination, 479 (2020) 114177, doi: 10.1016/j.desal.2019.114177.
[23] H. Abu Ali, M. Baronian, L. Burlace, P.A. Davies, S. Halasah, M. Hind, A. Hossain, C. Lipchin, A. Majali, M. Mark, Off-grid desalination for irrigation in the Jordan Valley, Desal. Water Treat., 168 (2019) 143–154.
[24] J.H. Lienhard, G.P. Thiel, D.M. Warsinger, L.D. Banchik, Low Carbon Desalination: Status and Research, Development, and Demonstration Needs, Report of a Workshop Conducted at the Massachusetts Institute of Technology in Association with the Global Clean Water Desalination Alliance, 2016.
[25] O. Igobo, Low-Temperature Isothermal Rankine Cycle for Desalination, Ph.D. Thesis, Aston University, Birmingham, UK, 2016.
[26] D.M. Warsinger, E.W. Tow, K.G. Nayar, L.A. Maswadeh, Energy efficiency of batch and semi-batch (CCRO) reverse osmosis desalination, Water Res., 106 (2016) 272–282.
[27] S. Jiang, Y. Li, B.P. Ladewig, A review of reverse osmosis membrane fouling and control strategies, Sci. Total Environ., 595 (2017) 567–583.
[28] J.W. Mullin, Crystallization, Butterworth-Heiman, London, 2001, pp. 86–134.
[29] S. Boerlage, Scaling and Particulate Fouling in Membrane Filtration Systems, CRC Press, Delft, 2001.
[30] H.-C. Flemming, Microbial Biofouling: Unsolved Problems, Insufficient Approaches, and Possible Solutions, in: Biofilm Highlights, Springer, Berlin, 2011, pp. 81–109.
[31] H. Shon, S. Vigneswaran, S.A. Snyder, Effluent organic matter (EfOM) in wastewater: constituents, effects, and treatment, Critical Rev. Environ. Sci. Technol., 36 (2006) 327–374.
[32] M. Al-Ahmad, F.A. Aleem, A. Mutiri, A. Ubaisy, Biofuoling in RO membrane systems Part 1: fundamentals and control, Desalination, 132 (2000) 173–179.
[33] X. Zhu, M. Elimelech, Fouling of reverse osmosis membranes by aluminum oxide colloids, J. Environ. Eng., 121 (1995) 884–892.
[34] C. Dai, A.G. Stack, A. Koishi, A. Fernandez-Martinez, S.S. Lee, Y. Hu, Heterogeneous nucleation and growth of barium sulfate at organic–water interfaces: interplay between surface hydrophobicity and Ba^{2+} adsorption, Langmuir, 32 (2016) 5277–5284.
[35] N. Dhakal, Reducing Consumption of Chemicals in Reverse Osmosis Systems, Institute for Water Education, UNESCO-IHE Delft, Netherlands, 2011.
[36] S. Lee, C. Boo, M. Elimelech, S. Hong, Comparison of fouling behavior in forward osmosis (FO) and reverse osmosis (RO), J. Membr. Sci., 365 (2010) 34–39.
[37] T. Nguyen, F.A. Roddick, L. Fan, Biofouling of water treatment membranes: a review of the underlying causes, monitoring techniques and control measures, Membranes, 2 (2012) 804–840.
[38] M. Jafari, A. D'haese, J. Zlopasa, E. Cornelissen, J.S. Vrouwenvelder, K. Verbeken, A. Verliefde, M. van Loosdrecht, C. Picioreanu, A comparison between chemical cleaning efficiency in lab-scale and full-scale reverse osmosis membranes: role of extracellular polymeric substances (EPS), J. Membr. Sci., 609 (2020) 118189, doi: 10.1016/j.memsci.2020.118189.
[39] B. Bendinger, H.H. Rijnaarts, K. Altendorf, A.J. Zehnder, Physicochemical cell surface and adhesive properties of coryneform bacteria related to the presence and chain length of mycolic acids, Appl. Environ. Microbiol., 59 (1993) 3973–3977.
[40] H.J. Busscher, A.H. Weerkamp, Specific and non-specific interactions in bacterial adhesion to solid substrata, FEMS Microbiol. Rev., 3 (1987) 165–173.
[41] R.A. Al-Juboori, T. Yusaf, Biofouling in RO system: mechanisms, monitoring and controlling, Desalination, 302 (2012) 1–23.
[42] J. Kramer, D. Tracey, The Solution to Reverse Osmosis Biofouling, Proceedings of IDA World Congress on Desalination and Water Use, 1995, pp. 33–44.
[43] H.F. Ridgway, H-C Flemming, Bacterial Adhesion and Fouling of Reverse Osmosis Membranes, Reverse Osmosis Technology, Marcel Dekker, New York, 1988, pp. 429–481.
[44] H.-C. Flemming, Reverse osmosis membrane biofouling, Exp. Therm. Fluid Sci., 14 (1997) 382–391.
[45] F.F. Abraham, Homogeneous Nucleation Theory, Academic Press, New York, 1974.
[46] A. Matin, F. Rahman, H.Z. Shafi, S.M. Zubair, Scaling of reverse osmosis membranes used in water desalination: phenomena, impact, and control; future directions, Desalination, 455 (2019) 135–157.
[47] K.D. Cobry, Z. Yuan, J. Gilron, V.M. Bright, W.B. Krantz, A.R. Greenberg, Comprehensive experimental studies of early-stage membrane scaling during nanofiltration, Desalination, 283 (2011) 40–51.
[48] N. Her, G. Amy, C. Jarusutthirak, Seasonal variations of nanofiltration (NF) foulants: identification and control, Desalination, 132 (2000) 143–160.
[49] H.-J. Lee, M.A. Halali, T. Baker, S. Sarathy, C.-F. De Lannoy, A comparative study of RO membrane scale inhibitors in wastewater reclamation: antiscalants versus pH adjustment, Separation and Purification Technology, 240 (2020) 116549, doi: 10.1016/j.seppur.2020.116549.
[50] H.-J. Oh, Y.-K. Choung, S. Lee, J.-S. Choi, T.-M. Hwang, J.H. Kim, Scale formation in reverse osmosis desalination: model development, Desalination, 238 (2009) 333–346.
[51] A.N. Quay, T. Tong, S.M. Hashmi, Y. Zhou, S. Zhao, M. Elimelech, Combined organic fouling and inorganic scaling in reverse osmosis: role of protein–silica interactions, Environ. Sci. Technol., 52 (2018) 9145–9153.
[52] T. Waly, Minimizing the Use of Chemicals to Control Scaling in SWRO: Improved Prediction of the Scaling Potential of Calcium Carbonate, UNESCO-IHE Institute for Water Education, Delft University of Technology, Taylor and Francis, Oxfordshire, United Kingdom, 2011.
[53] A.E. Nielsen, O. Söhnel, Interfacial tensions electrolyte crystal-aqueous solution, from nucleation data, J. Cryst. Growth, 11 (1971) 233–242.
[54] O. Söhnel, J.W. Mullin, Interpretation of crystallization induction periods, J. Colloid Interface Sci., 123 (1988) 43–50.
[55] S. Jiang, J.H. Ter Horst, Crystal nucleation rates from probability distributions of induction times, Cryst. Growth Des., 11 (2011) 256–261.
[56] C.Y. Tang, T. Chong, A.G. Fane, Colloidal interactions and fouling of NF and RO membranes: a review, Adv. Colloid Interface Sci., 164 (2011) 126–143.

[57] B. Derjaguin, L. Landau, Theory of the stability of strongly charged lyophobic sols and of the adhesion of strongly charged particles in solutions of electrolytes, Progr. Surf. Sci., 43 (1993) 30–59.
[58] J. Gregory, Particles in Water: Properties and Processes, CRC Press, Taylor and Francis, Oxfordshire, United Kingdom, 2005.
[59] J. Buffle, G.G. Leppard, Characterization of aquatic colloids and macromolecules. 1. Structure and behavior of colloidal material, Environ. Sci. Technol., 29 (1995) 2169–2175.
[60] J. Buffle, G. Leppard, Characterization of aquatic colloids and macromolecules. 2. Key role of physical structures on analytical results, Environ. Sci. Technol., 29 (1995) 2176–2184.
[61] J. Buffle, K.J. Wilkinson, S. Stoll, M. Filella, J. Zhang, A generalized description of aquatic colloidal interactions: the three-colloidal component approach, Environ. Sci. Technol., 32 (1998) 2887–2899.
[62] T. Berman, R. Mizrahi, C.G. Dosoretz, Transparent exopolymer particles (TEP): a critical factor in aquatic biofilm initiation and fouling on filtration membranes, Desalination, 276 (2011) 184–190.
[63] A. Fane, Ultrafiltration: factors influencing flux and rejection, Progr. Filtr. Sep., 4 (1986) 101–179.
[64] G. Belfort, B. Marx, Artificial particulate fouling of hyperfiltration membranes—II analysis and protection from fouling, Desalination, 28 (1979) 13–30.
[65] G. Belfort, F.W. Altena, Toward an inductive understanding of membrane fouling, Desalination, 47 (1983) 105–127.
[66] J. Gilron, D. Hasson, Calcium sulphate fouling of reverse osmosis membranes: flux decline mechanism, Chem. Eng. Sci., 42 (1987) 2351–2360.
[67] H.-C. Flemming, A. Tamachkiarowa, J. Klahre, J. Schmitt, Monitoring of fouling and biofouling in technical systems, Water Sci. Technol., 38 (1998) 291–298.
[68] I.S. Ngene, Real Time Visual Characterization of Membrane Fouling and Cleaning, University of Twente, Enschede, Netherlands, 2010, p. 115.
[69] H. Li, A.G. Fane, H.G. Coster, S. Vigneswaran, Direct observation of particle deposition on the membrane surface during crossflow microfiltration, J. Membr. Sci., 149 (1998) 83–97.
[70] H. Li, A. Fane, H. Coster, S. Vigneswaran, An assessment of depolarisation models of crossflow microfiltration by direct observation through the membrane, J. Membr. Sci., 172 (2000) 135–147.
[71] H. Li, A. Fane, H. Coster, S. Vigneswaran, Observation of deposition and removal behaviour of submicron bacteria on the membrane surface during crossflow microfiltration, J. Membr. Sci., 217 (2003) 29–41.
[72] J. Vrouwenvelder, J. Kruithof, Biofouling of Spiral Wound Membrane Systems, IWA Publishing, London, United Kingdom, 2011.
[73] J. Vrouwenvelder, J. Van Paassen, L. Wessels, A. Van Dam, S. Bakker, The membrane fouling simulator: a practical tool for fouling prediction and control, J. Membr. Sci., 281 (2006) 316–324.
[74] N. Siebdrath, W. Ding, E. Pietsch, J. Kruithof, W. Uhl, J.S. Vrouwenvelder, Construction and validation of a long-channel membrane test cell for representative monitoring of performance and characterization of fouling over the length of spiral-wound membrane modules, Desal. Water Treat., 89 (2017) 1–16.
[75] J. Vrouwenvelder, S. Manolarakis, J. Van der Hoek, J. Van Paassen, W.G.J. van der Meer, J. Van Agtmaal, H. Prummel, J. Kruithof, M. Van Loosdrecht, Quantitative biofouling diagnosis in full scale nanofiltration and reverse osmosis installations, Water Res., 42 (2008) 4856–4868.
[76] J. Vrouwenvelder, J. Van Paassen, J. Van Agtmaal, M. Van Loosdrecht, J. Kruithof, A critical flux to avoid biofouling of spiral wound nanofiltration and reverse osmosis membranes: fact or fiction?, J. Membr. Sci., 326 (2009) 36–44.
[77] J. Vrouwenvelder, D.G. Von Der Schulenburg, J. Kruithof, M. Johns, M. Van Loosdrecht, Biofouling of spiral-wound nanofiltration and reverse osmosis membranes: a feed spacer problem, Water Res., 43 (2009) 583–594.
[78] N.R. Sarker, A.M. Bilton, Real-time computational imaging of reverse osmosis membrane scaling under intermittent operation, J. Membr. Sci., 636 (2021) 119556, doi: 10.1016/j.memsci.2021.119556.
[79] M. Freire-Gormaly, A. Bilton, An experimental system for characterization of membrane fouling of solar photovoltaic reverse osmosis systems under intermittent operation, Desal. Water Treat., 73 (2017) 54–63.
[80] M. Freire-Gormaly, A. Bilton, Experimental quantification of the effect of intermittent operation on membrane performance of solar powered reverse osmosis desalination systems, Desalination, 435 (2018) 188–197.
[81] M. Pontié, S. Rapenne, A. Thekkedath, J. Duchesne, V. Jacquemet, J. Leparc, H. Suty, Tools for membrane autopsies and antifouling strategies in seawater feeds: a review, Desalination, 181 (2005) 75–90.
[82] F. Butt, F. Rahman, U. Baduruthamal, Identification of scale deposits through membrane autopsy, Desalination, 101 (1995) 219–230.
[83] L. Fortunato, A.H. Alshahri, A.S. Farinha, I. Zakzouk, S. Jeong, T. Leiknes, Fouling investigation of a full-scale seawater reverse osmosis desalination (SWRO) plant on the Red Sea: membrane autopsy and pretreatment efficiency, Desalination, 496 (2020) 114536, doi: 10.1016/j.desal.2020.114536.
[84] X. Li, H. Zhang, Y. Hou, Y. Gao, J. Li, W. Guo, H.H. Ngo, In situ investigation of combined organic and colloidal fouling for nanofiltration membrane using ultrasonic time domain reflectometry, Desalination, 362 (2015) 43–51.
[85] X. Li, J. Li, J. Wang, H. Zhang, Y. Pan, In situ investigation of fouling behavior in submerged hollow fiber membrane module under sub-critical flux operation via ultrasonic time domain reflectometry, J. Membr. Sci., 411 (2012) 137–145.
[86] X. Li, J. Li, J. Wang, H. Wang, C. Cui, B. He, H. Zhang, Direct monitoring of sub-critical flux fouling in a horizontal double-end submerged hollow fiber membrane module using ultrasonic time domain reflectometry, J. Membr. Sci., 451 (2014) 226–233.
[87] Z. Zhang, V.M. Bright, A.R. Greenberg, Use of capacitive microsensors and ultrasonic time-domain reflectometry for in-situ quantification of concentration polarization and membrane fouling in pressure-driven membrane filtration, Sens. Actuators, B, 117 (2006) 323–331.
[88] H.-C. Flemming, G. Schaule, R. McDonogh, H.F. Ridgway, Effects and Extent of Biofilm Accumulation in Membrane Systems, Biofouling and Biocorrosion in Industrial Water Systems, Springer Publishing, New York City, United States of America, 1994, pp. 63–89.
[89] A. Siddiqui, I. Pinel, E. Prest, S. Bucs, M. van Loosdrecht, J. Kruithof, J.S. Vrouwenvelder, Application of DBNPA dosage for biofouling control in spiral wound membrane systems, Desal. Water Treat., 68 (2017) 12–22.
[90] N. Farhat, J.S. Vrouwenvelder, M.C. Van Loosdrecht, S.S. Bucs, M. Staal, Effect of water temperature on biofouling development in reverse osmosis membrane systems, Water Res., 103 (2016) 149–159.
[91] F. Beyer, J. Laurinonyte, A. Zwijnenburg, A.J. Stams, C.M. Plugge, Membrane fouling and chemical cleaning in three full-scale reverse osmosis plants producing demineralized water, J. Eng., 2017 (2017) 6356751, doi: 10.1155/2017/6356751.
[92] S. Gare, RO systems: the importance of pre-treatment, Filtr. Sep., 39 (2002) 22–27.
[93] A. Matin, T. Laoui, W. Falath, A.M. Farooque, Fouling control in reverse osmosis for water desalination & reuse: current practices & emerging environment-friendly technologies, Sci. Total Environ., 765 (2020) 142721, doi: 10.1016/j.scitotenv.2020.142721.
[94] J.K. Edzwald, J. Haarhoff, Seawater pretreatment for reverse osmosis: chemistry, contaminants, and coagulation, Water Res., 45 (2011) 5428–5440.
[95] P.N. Johnson, A. Amirtharajah, Ferric chloride and alum as single and dual coagulants, J. Am. Water Works Assoc., 75 (1983) 232–239.
[96] J. Duan, J. Wang, N. Graham, F. Wilson, Coagulation of humic acid by aluminium sulphate in saline water conditions, Desalination, 150 (2002) 1–14.

[97] M. Umar, F. Roddick, L. Fan, Comparison of coagulation efficiency of aluminium and ferric-based coagulants as pre-treatment for UVC/H_2O_2 treatment of wastewater RO concentrate, Chem. Eng. J., 284 (2016) 841–849.
[98] N.K. Shammas, Coagulation and Flocculation, Humana Press, Totowa, 2005, pp. 103–139.
[99] S.A.A. Tabatabai, J.C. Schippers, M.D. Kennedy, Effect of coagulation on fouling potential and removal of algal organic matter in ultrafiltration pretreatment to seawater reverse osmosis, Water Res., 59 (2014) 283–294.
[100] J. Kavitha, M. Rajalakshmi, A. Phani, M. Padaki, Pretreatment processes for seawater reverse osmosis desalination systems—a review, J. Water Process Eng., 32 (2019) 100926, doi: 10.1016/j.jwpe.2019.100926.
[101] S.M. Korotta-Gamage, A. Sathasivan, A review: potential and challenges of biologically activated carbon to remove natural organic matter in drinking water purification process, Chemosphere, 167 (2017) 120–138.
[102] E. Bar-Zeev, N. Belkin, B. Liberman, T. Berman, I. Berman-Frank, Rapid sand filtration pretreatment for SWRO: microbial maturation dynamics and filtration efficiency of organic matter, Desalination, 286 (2012) 120–130.
[103] L. Huisman, W.E. Wood, Slow Sand Filtration, World Health Organization, WHO Press, Geneva, Switzerland, 1974.
[104] A. Alhadidi, A.J. Kemperman, R. Schurer, J. Schippers, M. Wessling, W.G.J. van der Meer, Using SDI, SDI+ and MFI to evaluate fouling in a UF/RO desalination pilot plant, Desalination, 285 (2012) 153–162.
[105] G. Pearce, S. Talo, K. Chida, A. Basha, A. Gulamhusein, Pretreatment options for large scale SWRO plants: case studies of trials at Kindasa, Saudi Arabia, and conventional pretreatment in Spain, Desalination, 167 (2004) 175–189.
[106] D.F. Halpern, J. McArdle, B. Antrim, UF pretreatment for SWRO: pilot studies, Desalination, 182 (2005) 323–332.
[107] M. Busch, R. Chu, U. Kolbe, Q. Meng, S. Li, Ultrafiltration pretreatment to reverse osmosis for seawater desalination—three years field experience in the Wangtan Datang power plant, Desal. Water Treat., 10 (2009) 1–20.
[108] S. Van Hoof, A. Hashim, A. Kordes, The effect of ultrafiltration as pretreatment to reverse osmosis in wastewater reuse and seawater desalination applications, Desalination, 124 (1999) 231–242.
[109] A.M. Farooque, A.M. Hassan, A. Al-Amoudi, Autopsy and Characterisation of NF Membranes after Long-Term Operation in a NF-SWRO Pilot Plant, IDA World Congress on Desalination and Water Reuse, San Diego, CA, 1999.
[110] A. Hassan, A. Farooque, A. Jamaluddin, A. Al-Amoudi, M. Al-Sofi, A. Al-Rubaian, N. Kither, I. Al-Tisan, A. Rowaili, A demonstration plant based on the new NF-SWRO process, Desalination, 131 (2000) 157–171.
[111] A.S. Al-Amoudi, A.M. Farooque, Performance restoration and autopsy of NF membranes used in seawater pretreatment, Desalination, 178 (2005) 261–271.
[112] A.A. Al-Hajouri, A.S. Al-Amoudi, A.M. Farooque, Long term experience in the operation of nanofiltration pretreatment unit for seawater desalination at SWCC SWRO plant, Desal. Water Treat., 51 (2013) 1861–1873.
[113] S. Haig, G. Collins, R. Davies, C. Dorea, C. Quince, Biological aspects of slow sand filtration: past, present and future, Water Sci. Technol.: Water Supply, 11 (2011) 468–472.
[114] F.F. de Oliveira, R.P. Schneider, Slow sand filtration for biofouling reduction in seawater desalination by reverse osmosis, Water Res., 155 (2019) 474–486.
[115] S. Jamaly, N. Darwish, I. Ahmed, S. Hasan, A short review on reverse osmosis pretreatment technologies, Desalination, 354 (2014) 30–38.
[116] A.F. Corral, U. Yenal, R. Strickle, D. Yan, E. Holler, C. Hill, W.P. Ela, R.G. Arnold, Comparison of slow sand filtration and microfiltration as pretreatments for inland desalination via reverse osmosis, Desalination, 334 (2014) 1–9.
[117] W. Song, V. Ravindran, B.E. Koel, M. Pirbazari, Nanofiltration of natural organic matter with H_2O_2/UV pretreatment: fouling mitigation and membrane surface characterization, J. Membr. Sci., 241 (2004) 143–160.
[118] Y. Jin, H. Lee, M. Zhan, S. Hong, UV radiation pretreatment for reverse osmosis (RO) process in ultrapure water (UPW) production, Desalination, 439 (2018) 138–146.
[119] W. Han, P. Zhang, W. Zhu, J. Yin, L. Li, Photocatalysis of p-chlorobenzoic acid in aqueous solution under irradiation of 254 nm and 185 nm UV light, Water Res., 38 (2004) 4197–4203.
[120] D. Cassan, B. Mercier, F. Castex, A. Rambaud, Effects of medium-pressure UV lamps radiation on water quality in a chlorinated indoor swimming pool, Chemosphere, 62 (2006) 1507–1513.
[121] W. Collentro, A novel approach to control microbial fouling of reverse osmosis elements, Ultrapure Water J., 31 (2014) 27–34.
[122] H.A. Di Martino Patrick, H. Ahmed, H. Véronique, M. Cyril, Assessment of UV Pre-Treatment to Reduce Fouling of NF Membranes, R.Y. Ning, Ed., Expanding Issues in Desalination, 2011, p. 219, doi: 10.5772/22462. Available at: https://www.intechopen.com/chapters/20351
[123] H.-N.G. Company, Chemical Pretreatment for RO and NF, H.-N.G. Company (Ed.), California, United States of America, 2013.
[124] E. Darton, Scale inhibition techniques used in membrane systems, Desalination, 113 (1997) 227–229.
[125] E.K. Zeiher, B. Ho, K.D. Williams, Novel antiscalant dosing control, Desalination, 157 (2003) 209–216.
[126] H. Li, W. Liu, X. Qi, Evaluation of a novel $CaSO_4$ scale inhibitor for a reverse osmosis system, Desalination, 214 (2007) 193–199.
[127] M.K. Shahid, M. Pyo, Y.-G. Choi, The operation of reverse osmosis system with CO2 as a scale inhibitor: a study on operational behavior and membrane morphology, Desalination, 426 (2018) 11–20.
[128] M. Schönbächler, M. Fehr, Basics of Ion Exchange Chromatography for Selected Geological Applications, Treatise on Geochemistry, Vol. 15: Analytical Geochemistry/Inorganic Instrument Analysis, Elsevier, 2013, pp. 124–146.
[129] G. Klein, T.J. Jarvis, T. Vermeulen, Fluidized-bed ion exchange with precipitation-principles and bench-scale development, Recent Dev. Sep. Sci., 5 (1979) 185–198.
[130] T. Vermeulen, B.W. Tleimat, G. Klein, Ion-exchange pretreatment for scale prevention in desalting systems, Desalination, 47 (1983) 149–159.
[131] G. Klein, Design and Development of Cyclic Operations, Percolation Processes: Theory and Applications, Sijthoff & Noordhoff Alphen aan den Rijn, Netherlands, 1981, pp. 427–441.
[132] A. Venkatesan, P.C. Wankat, Simulation of ion exchange water softening pretreatment for reverse osmosis desalination of brackish water, Desalination, 271 (2011) 122–131.
[133] A. Zhu, Energy and Cost Optimization of Reverse Osmosis Desalination, University of California, Los Angeles, 2012.
[134] M. Futterlieb, I.M. ElSherbiny, M. Tuczinski, J. Lipnizki, S. Panglisch, Limits of high recovery inland desalination: closed-circuit reverse osmosis–a viable option?, Chemie Ingenieur Technik, 93 (2021) 1359–1368.
[135] D. Kim, S. Jung, J. Sohn, H. Kim, S. Lee, Biocide application for controlling biofouling of SWRO membranes—an overview, Desalination, 238 (2009) 43–52.
[136] N. Nagaraja, L. Skillman, Z. Xie, S. Jiang, G. Ho, D. Li, Investigation of compounds that degrade biofilm polysaccharides on reverse osmosis membranes from a full-scale desalination plant to alleviate biofouling, Desalination, 403 (2017) 88–96.
[137] B.S. Oh, H.Y. Jang, J. Cho, S. Lee, E. Lee, I.S. Kim, T.M. Hwang, J.-W. Kang, Effect of ozone on microfiltration as a pretreatment of seawater reverse osmosis, Desalination, 238 (2009) 90–97.
[138] M. Boorsma, S. Dost, S. Klinkhamer, J. Schippers, Monitoring and controlling biofouling in an integrated membrane system, Desal. Water Treat., 31 (2011) 347–353.
[139] D.A. Caron, M.-È. Garneau, E. Seubert, M.D. Howard, L. Darjany, A. Schnetzer, I. Cetinić, G. Filteau, P. Lauri,

B. Jones, Harmful algae and their potential impacts on desalination operations off southern California, Water Res., 44 (2010) 385–416.
[140] G.S. Ibrahim, A.M. Isloor, R. Farnood, Reverse Osmosis Pretreatment Techniques, Fouling, and Control Strategies, Current Trends and Future Developments on (Bio-) Membranes, Elsevier, Mangalore, 2020, pp. 165–186.
[141] S. Lattemann, T. Höpner, Environmental impact and impact assessment of seawater desalination, Desalination, 220 (2008) 1–15.
[142] J. Redondo, I. Lomax, Experiences with the pretreatment of raw water with high fouling potential for reverse osmosis plant using FILMTEC membranes, Desalination, 110 (1997) 167–182.
[143] H.K. Khordagui, A conceptual approach to selection of a control measure for residual chlorine discharge in Kuwait Bay, Environ. Manage., 16 (1992) 309–316.
[144] N. Farhat, E. Loubineaud, E. Prest, J. El-Chakhtoura, C. Salles, S.S. Bucs, J. Trampé, W. Van den Broek, J. Van Agtmaal, M. Van Loosdrecht, Application of monochloramine for wastewater reuse: effect on biostability during transport and biofouling in RO membranes, J. Membr. Sci., 551 (2018) 243–253.
[145] M.K. da Silva, I.C. Tessaro, K. Wada, Investigation of oxidative degradation of polyamide reverse osmosis membranes by monochloramine solutions, J. Membr. Sci., 282 (2006) 375–382.
[146] Z. Yin, T. Wen, Y. Li, A. Li, C. Long, Alleviating reverse osmosis membrane fouling caused by biopolymers using pre-ozonation, J. Membr. Sci., 595 (2020) 117546, doi: 10.1016/j.memsci.2019.117546.
[147] Z. Yin, T. Wen, Y. Li, A. Li, C. Long, Pre-ozonation for the mitigation of reverse osmosis (RO) membrane fouling by biopolymer: the roles of Ca^{2+} and Mg^{2+}, Water Res., 171 (2020) 115437, doi: 10.1016/j.watres.2019.115437.
[148] C.L. Murray-Gulde, J.E. Heatley, A.L. Schwartzman, J.H. Rodgers Jr., Algicidal effectiveness of clearigate, cutrine-plus, and copper sulfate and margins of safety associated with their use, Arch. Environ. Contam. Toxicol., 43 (2002) 19–27.
[149] F.S. Al Ketbi, E.Z. Isnasious, A.M. Al Mahyas, Practical observations on reverse osmosis plants including raw water contamination problems, different intake stations and permeator performance, Desalination, 93 (1993) 259–272.
[150] G.Z. Ramon, T.-V. Nguyen, E.M. Hoek, Osmosis-assisted cleaning of organic-fouled seawater RO membranes, Chem. Eng. J., 218 (2013) 173–182.
[151] A. Dana, S. Hadas, G.Z. Ramon, Potential application of osmotic backwashing to brackish water desalination membranes, Desalination, 468 (2019) 114029, doi: 10.1016/j.desal.2019.05.012.
[152] E. Bar-Zeev, M. Elimelech, Reverse osmosis biofilm dispersal by osmotic back-flushing: cleaning via substratum perforation, Environ. Sci. Technol. Lett., 1 (2014) 162–166.
[153] M. Ando, S. Ishihara, K. Ishii, Spiral Wound Membrane Element, Spiral Wound Membrane Module and Treatment System Employing the Same as Well as Running Method and Washing Method Therefor, EU Patent, EP1174177A3, 2004.
[154] M. Ando, K. Ishii, S. Ishihara, Running Method and Treatment System for Spiral Wound Membrane Element and Spiral Wound Membrane Module, United States Patent, US-0899649, 2001.
[155] K. Spiegler, J. Macleish, Molecular (osmotic and electro-osmotic) backwash of cellulose acetate hyperfiltration membranes, J. Membr. Sci., 8 (1981) 173–192.
[156] S. Daly, A. Allen, V. Koutsos, A.J. Semião, Influence of organic fouling layer characteristics and osmotic backwashing conditions on cleaning efficiency of RO membranes, J. Membr. Sci., 616 (2020) 118604.
[157] J.-J. Qin, M.H. Oo, K.A. Kekre, B. Liberman, Development of novel backwash cleaning technique for reverse osmosis in reclamation of secondary effluent, J. Membr. Sci., 346 (2010) 8–14.
[158] A. Sagiv, R. Semiat, Backwash of RO spiral wound membranes, Desalination, 179 (2005) 1–9.
[159] N.Y. Yip, M. Elimelech, Influence of natural organic matter fouling and osmotic backwash on pressure retarded osmosis energy production from natural salinity gradients, Environ. Sci. Technol., 47 (2013) 12607–12616.
[160] Y.-H. Cai, A.I. Schäfer, Renewable energy powered membrane technology: Impact of solar irradiance fluctuation on direct osmotic backwash, J. Membr. Sci., 598 (2020) 117666.
[161] J. Gilron, E. Korin, Method and System for Increasing Recovery and Preventing Precipitation Fouling in Pressure-Driven Membrane Processes, United States Patent, US9649598B2, 2012.
[162] N. Pomerantz, Y. Ladizhansky, E. Korin, M. Waisman, N. Daltrophe, J. Gilron, Prevention of scaling of reverse osmosis membranes by "zeroing" the elapsed nucleation time. Part I. Calcium sulfate, Ind. Eng. Chem. Res., 45 (2006) 2008–2016.
[163] J. Gilron, M. Waisman, N. Daltrophe, N. Pomerantz, M. Milman, I. Ladizhansky, E. Korin, Prevention of precipitation fouling in NF/RO by reverse flow operation, Desalination, 199 (2006) 29–30.
[164] M. Uchymiak, A.R. Bartman, N. Daltrophe, M. Weissman, J. Gilron, P.D. Christofides, W.J. Kaiser, Y. Cohen, Brackish water reverse osmosis (BWRO) operation in feed flow reversal mode using an ex situ scale observation detector (EXSOD), J. Membr. Sci., 341 (2009) 60–66.
[165] G. Mizrahi, K. Wong, X. Lu, E. Kujundzic, A.R. Greenberg, J. Gilron, Ultrasonic sensor control of flow reversal in RO desalination. Part 2: mitigation of calcium carbonate scaling, J. Membr. Sci., 419 (2012) 9–19.
[166] X. Lu, E. Kujundzic, G. Mizrahi, J. Wang, K. Cobry, M. Peterson, J. Gilron, A.R. Greenberg, Ultrasonic sensor control of flow reversal in RO desalination—Part 1: mitigation of calcium sulfate scaling, J. Membr. Sci., 419 (2012) 20–32.
[167] D. Tang, J. Song, A.W.-K. Law, Application of feed flow reversal for nanofiltration of highly concentrated industrial wastewaters, Desalination, 485 (2020) 114462, doi: 10.1016/j.desal.2020.114462.
[168] O. Söhnel, J. Garside, Precipitation: Basic Principles and Industrial Applications, Butterworth-Heinemann, Oxford, 1992.
[169] S. He, J.E. Oddo, M.B. Tomson, The nucleation kinetics of calcium sulfate dihydrate in NaCl solutions up to 6 m and 90 C, J. Colloid Interface Sci., 162 (1994) 297–303.
[170] F. Alimi, H. Elfil, A. Gadri, Kinetics of the precipitation of calcium sulfate dihydrate in a desalination unit, Desalination, 158 (2003) 9–16.
[171] M.Y. Ashfaq, M.A. Al-Ghouti, D.A. Da'na, H. Qiblawey, N. Zouari, Effect of concentration of calcium and sulfate ions on gypsum scaling of reverse osmosis membrane, mechanistic study, J. Mater. Res. Technol., 9 (2020) 13459–13473.
[172] T. Kennedy, R. Merson, B. McCoy, Improving permeation flux by pulsed reverse osmosis, Chem. Eng. Sci., 29 (1974) 1927–1931.
[173] I. Liberman, B. Liberman, Forward Osmotic and Water Hammer Method of Membrane Cleaning, United States Patent, US10507432B2, 2019.
[174] K. Choon Ng, T. Missimer, G. Amy, Processes and Apparatus for Inhibiting Bio-Fouling, United States Patent, US20120318731A1, 2012.
[175] B. Liberman, L. Eshed, G. Greenberg, Pulse flow RO – the new RO technology for waste and brackish water applications, Desalination, 479 (2020) 114336, doi: 10.1016/j.desal.2020.114336.